SES6-CT-2003-502705

RENEW

Renewable fuels for advanced powertrains

Integrated Project

Sustainable energy systems

Scientific report
WP5.5
Thermochemical gaseous fuel producion

Period covered	from:	01.01.04	to: 31.12.07	Date of preparation	27.03.08
Start date of project:		01-01-04		Duration:	48 months

Authors: S. Biollaz (work packed leader), M.C. Seemann, T.J. Schildhauer, I. Czekaj, F. Raimondi

Project coordinator name: Dr. Frank Seyfried

Project coordinator organisation name: VOLKSWAGEN AG
Berliner Ring 2

38436 Wolfsburg

Revision (draft 1)

Scientific Report WP5.5

Thermochemical gaseous fuel producion

Project leader: S. Biollaz

Co-Authors: M.C. Seemann, T.J. Schildhauer, I. Czekaj, F. Raimondi

Table of contents

I. Theoretical Analysis

1.Introduction 3

1.1.Challenges of Methanation 3

2. Evaluation of Gasification technologies for Methanation 7

2.1. Technology overview 7

2.2. Characterization of the gas composition 9

3.Case study for FICFB gasification system and methanation 11

3.1. Experimental proof of equilibrium calculations 11

3.2. Determination of the most promising conditions for methanation 11

3.3. Case FICFB 12

3.4. Results 14

3.5. Producer gas composition and overall chemical efficiency 15

II. Proof of concept for gaseous fuel production, using a slip stream of the FICFB gasifier in Güssing

1. Introduction 18

Results of previous work 18

2. Design and Construction 20

2.1 Methanation unit 20

2.2 Analytics 21

2.3 Control unit 22

3. First tests and experiments at PSI 23

3.1 Variation of temperature and pressure 23

3.2 Long duration test at PSI 24

3.3 Experimental simulation of a two stage methanation 24

4. First long duration tests in Güssing 2004 25
4.1 Experiment COSYMA_3 (October 2004) 26
4.2 Experiment COSYMA_4 (November 2004) 28
4.3 Experiment COSYMA_16 (Spring 2007) 28
5. Intermediate conclusions 30
6. Detailed post-test analyses of catalyst samples 31
6.1 Temperature programmed Oxidation (TPO) 31
6.2 XANES 32
6.3 Catalyst characterisation by XPS 33
7. Axial gas phase concentration profiles in the methanation reactor 37
7.1 Experimental 37
7.2 Results and discussion 38
8. Experiments including the HDS unit in 2005 44
8.1 Overview over the experiments 44
8.2 Results of TPO analyses and discussion 45

III. Conclusions 46
IV. References 48
V. Publications 49

I. Theoretical Analysis

1. Introduction

The conversion of biomass to SNG can be structured roughly into four main units; gasification, raw gas cleaning, fuel synthesis and gas upgrading. In figure 1, the basic scheme of a SNG production plant is shown. A solid feed is thermally converted to a raw gas, cleaned of particles, tars and sulphur. In the fuel synthesis the raw gas is converted into raw SNG (a CH_4/CO_2 mixture) that is cleaned from CO_2 and optionally H_2 (gas upgrading) before injection into the natural gas grid.

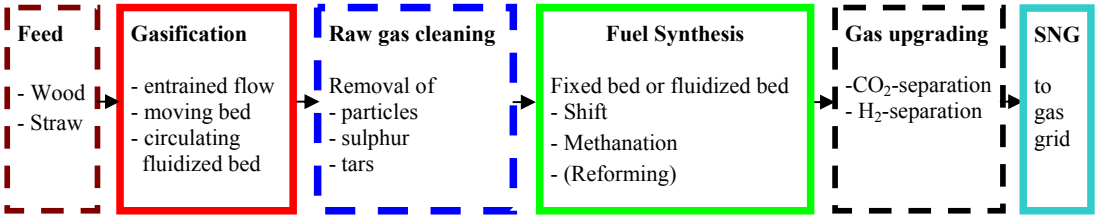

Figure 1: The basic scheme of a SNG production plant for the conversion of biomass into SNG

This general analysis described in this deliverable focuses on the two conversion steps relevant for the overall chemical efficiency of the process; the gasification (process) and the fuel synthesis, incorporating the water-gas-shift (WGS) (eq. 2) to adjust the H_2/CO-ratio and methanation (eq. 1).

$$CO + 3\ H_2 \rightarrow CH_4 + H_2O \qquad (1)$$

$$CO + H_2O \rightarrow CO_2 + H_2 \qquad (2)$$

The key for the realization of an efficient SNG production is a high compatibility of the gasification and synthesis units and a good adjustment of the reaction conditions to the raw gas composition.

1.1. Challenges of Methanation

In figure 2, the HHV versus relative density diagram, changes are displayed from raw gas to SNG. The steps are the WGS to adjust the H_2/CO-ratio (1->1b), the methanation (1b->2) and the CO_2 separation (2->3). Alternatively the first two steps can be performed simultaneously in a fluidized bed methanation (1->2). For the fuel synthesis resp. methanation there are four main challenges to overcome:

Requirements for the natural gas grid

As an example for quality targets the rules of the German Technical and Scientific Association for Gas and Water (DVGW G 260) [DVGW,2000] are shown in figure 2. The required gas specification is defined by a hexagonal area plotted in a diagram showing the relative density d versus the higher heating value (HHV) of the gas. Relevant for a countrywide applicable technology are the standards of the premium quality gas (H-gas) that is distributed in wide parts of Germany. In this rule, furthermore, the tolerable amount of contaminants like O_2, CO_2, H_2, and H_2S are set. Limits for contaminants such as CO, NH_3 do not exist yet and the discussion about appropriate limits is still under way (DVGW G 262) [DVGW,-]. In this work a concentration of 0.5% as limit for CO is assumed.

Carbon deposition on the methanation catalyst ($H_2/CO<3$)

One major handicap of raw gases is the insufficient gas composition, i.e. the H_2 to CO ratio. Without good adjustment of the reaction conditions the catalyst will deactivate rapidly due to carbon formation.

The problem can be displayed easily by placing the producer gases in a ternary CHO diagram (figure 3). The diagram is divided by an isotherm based on equilibrium calculations (320°C) into two regions. Above the isotherm carbon deposition on the catalyst is thermodynamically favoured. Below the isotherm carbon free conversion of the producer gas is expected.

Solid feedstocks such as biomass and coal are placed in the left half of the triangle clearly in the carbon deposition region. As H_2O and O_2 is added in the gasification process and converted to H_2, CO and CO_2 the conversion moves the atomic composition closer to the isotherm. However, synthesis of SNG without the risk of carbon deposition is not possible in this region of the diagram. To avoid the carbon deposition region, more H_2O must be added to shift the atomic composition into the carbon deposition free region.

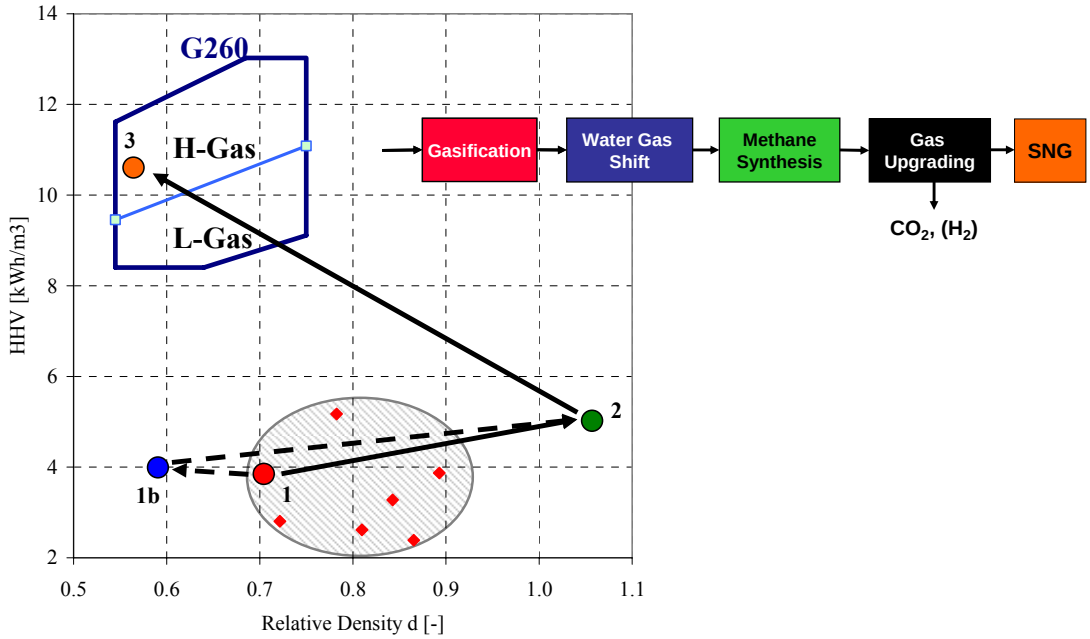

Figure 2: Illustration of changing gas compositions in a HHV relative density d diagram:
Standard route: 1→1b shift to $H_2/CO = 3/1$
1b→2 methanation (fixed bed)
2→3 CO_2-separation
Alternative route: 1→2 integrated shift and methanation (fluidized bed)

The adjustment of the H_2/CO-ratio can be done either in a separate WGS-unit (1->1b) or alternatively directly in a fluidized bed methanation featuring the internal shift (1->2). The simultaneous shift and methanation was shown in the COMFLUX [Hedden,1986] project.
However, the thermodynamic calculations can only exhibit rough guidelines for the design of the process as carbon deposition is a process strongly influenced by kinetics. For that reason, not only an insufficient H_2/CO-ratio but also the presence of higher hydrocarbons (HC) in the raw gas is a risk.

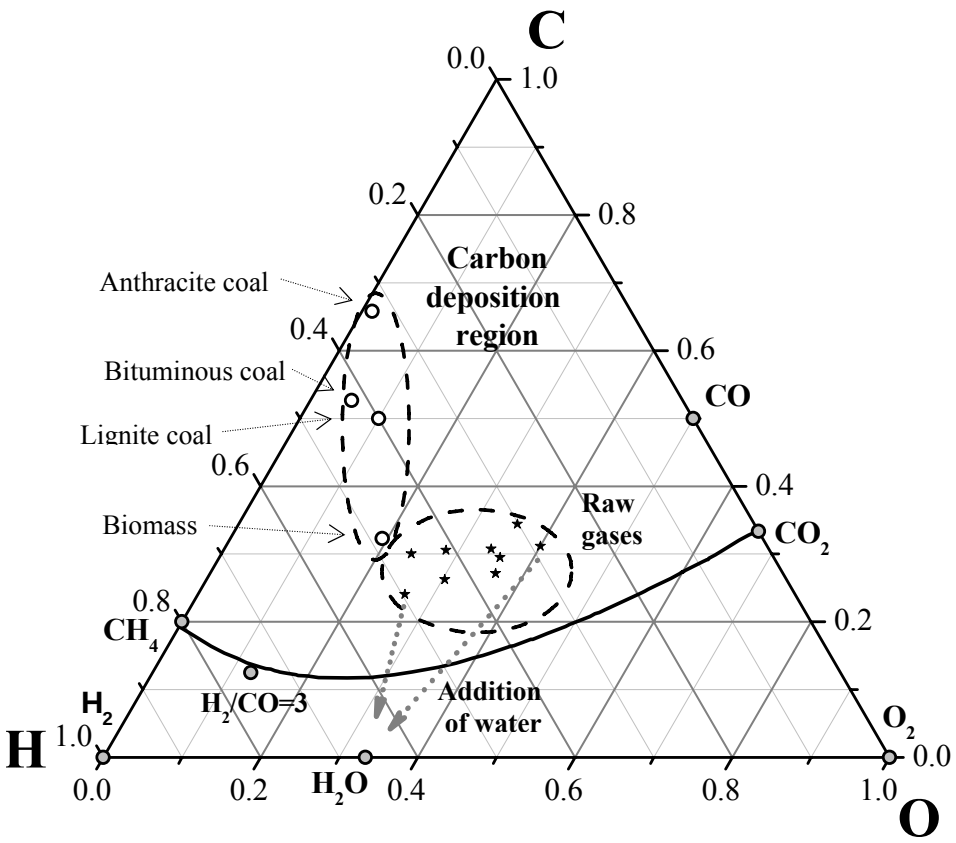

Figure 3: Positioning of the atomic composition of different raw gases and feedstocks in the triangular CHO diagram. The diagram is separated by an isotherm (320°C) into carbon deposition region and a region where thermodynamically no solid carbon is expected. The atomic compositions of the feedstock is situated in the left upper half, the atomic composition of the raw gases is situated close to the centre of the triangle still into the carbon deposition region.

"Tar" tolerance of the catalyst

The higher HC/tars in the gas increase the risk of carbon deposition as they tend to form carbon by polymerization on the catalyst surface. Most of the hydrocarbons are aromatic structure and originate from the devolatilisation of the feedstock. These higher hydrocarbons are classified into GC- undetectable, heavy poly aromatic (i.e. Flouranthene), light poly aromatic (i.e. Naphthalene), light aromatic (i.e. Toluene), and water soluble compounds and heterocyclic (i.e. Phenol, Pyridine) tars [Devi,2005]. In our work, the tars are classified into heavy tars and light tars like Benzene, Toluene and Naphthalene. In raw gases cleaned by scrubbing at ambient conditions only the latter group is present

The challenge is to remove or reform the tars to a degree that carbon formation is avoided. If the tars can be reformed in the fluidized bed of the methanation, they can be even considered as "fuel" for the SNG production.

Sulphur tolerance

Nickel is the most common metal used for commercial methanation catalysts. As sulphur forms

strong bonds with nickel and deactivates the catalyst, a solid sulphur removal is required to guarantee a long catalyst lifetime. Depending on the catalyst, the sulphur content of the gas should be in the range of 0.1 to 1 ppm.

2. Evaluation of Gasification technologies for Methanation

Gasification is a technology that converts solid carbonaceous materials, such as biomass or coal, into a combustible gas mixture. When the material is heated up, volatiles are released (devolatilisation) and char is produced. The char reacts with CO_2 and steam to produce carbon monoxide and hydrogen. All these processes are endothermic and additional heat is needed to support the gasification. In case the process is heated externally, the gasification process is called allothermic. For autothermal gasification, oxygen is added to raise heat by combusting the volatile products and some of the char. The resulting gas of any gasification process is a raw gas. The autothermal gasification process can be roughly described by two reactions, the exothermic combustion (6) and the endothermic gasification (eq.7) [1950, Kaup,, Skov,1974].

$$CH_xO_y + O_2 \rightarrow CO_2 + H_2O \quad (3)$$

$$CH_xO_y + H_2O \rightarrow CO + H_2 \quad (4)$$

Actually, the autothermal gasification can be viewed as an imperfect combustion or partial oxidation. The value that defines the share of carbonaceous material that is combusted and the share that is gasified is called lambda, λ. Lambda is defined as the ratio of oxygen added to the oxygen needed for a stoichiometric complete combustion of the feedstock to CO_2 and water.

$$\lambda = \frac{\text{oxygen added}}{\text{stoichiometric amount of oxygen}} \quad (5)$$

The chemical efficiency of a gasification system, η_{chG} is defined by the Lower Heating Value (LHV) of the feed and the LHV of the producer gas (eq. 9).

$$\eta_{ch\,G} = \frac{LHV_{Producer\,gas}\ \dot{n}_{Producer\,gas}}{LHV_{Feed}\ \dot{n}_{Feed}} \quad (6)$$

The aim of any gasification technology is the transformation of chemical energy from the solid feedstock into the producer gas with the highest efficiency. This means, keeping λ as low as possible to minimize the losses of chemical energy due to the combustion.

2.1. Gasification technology overview

In literature a broad variety of gasification technologies have been described. Possible

candidates as producers of synthesis gas for the methanation from biomass are presented here. The operating parameters and the applied technology of the gasifiers are given in table 3. The range of temperature and pressure varies between 800 - 1400°C and 1 - 20 bara respectively. Nonetheless, all gasifier presented here have one thing in common; they produce an almost nitrogen-free producer gas. As nitrogen is difficult to separate from methane this attribute is essential. Therefore, the gasifiers are either oxygen blown, or use the technique of the indirect gasification.

Table 1: Operation parameters of different gasifiers

		CFB	FICFB	GSP	Carbo-V
Feedstock		Biomass			
Technology		circulating	indirect	entrained flow	
Temp.	[°C]	950-1000	850	1200-1400	1000
Pres.	[bara]	20	1	25	5
Oxidant		oxygen	steam/air	oxygen	oxygen

Within this overview three principal technologies are differentiated; the entrained flow, the circulating fluidized bed and the indirect gasification technology.

GSP and Carbo-V are entrained flow gasifiers. These systems typically run at high temperatures and pressures leading to a low output of HC. As they form a slag coating at their inner wall they are suitable for fuels with high ash content and low melting point. The Gaskombinat Schwarze Pumpe (GSP) gasifier [Kirmse,2000, Eckert,1998, Rehwinkel,1990] has been developed for coal gasification, but can be fed with a mixture of pyrolysis oil and coke, derived from biomass pyrolysis, i.e. straw (figure 7).

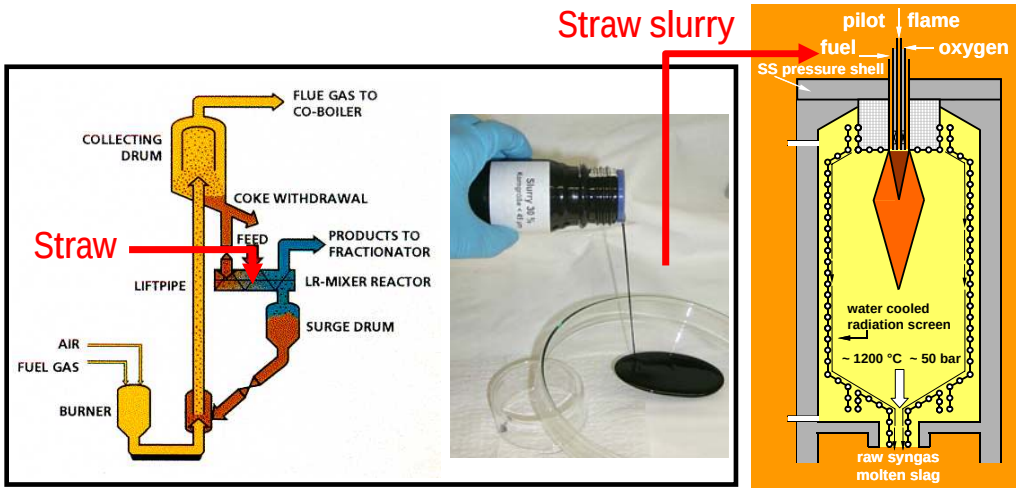

Figure 4: Two step process of pyrolysis and gasification of the slurry developed in cooperation of FZK and Future Energy (Freiberg, Germany)

Another entrained flow system adapted to use biomass is the Carbo-V gasifier [Biollaz,2006, Wolf,2001].

As an example for a biomass-fed circulation fluidized bed (CFB) gasifer, the plant in Värnamo (Sweden) is included (figure 8). In the CHRISGAS project of the EU the gasifier will be modified to oxygen-steam-blown operation to produce nitrogen-free raw gas [Stahl,2005]. The gas composition used in this overview is a projected gas composition [Albertazzi,2005].

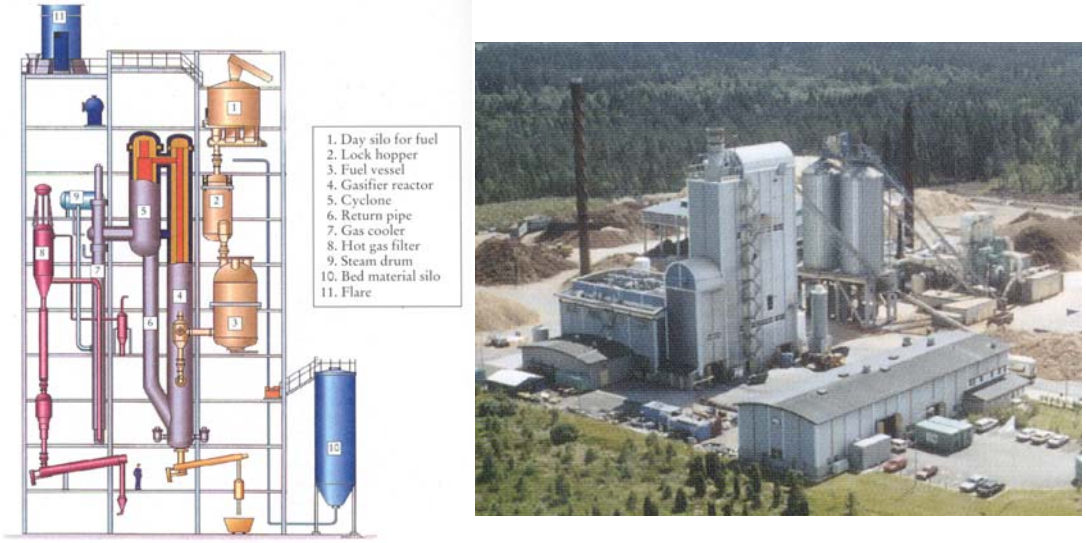

Figure 5: Circulating fluidized bed gasification system (Foster Wheeler) in Värnamo (Schweden). Within the CHRISGAS project the system is modified from air-blown to oxygen-steam-blown operation.

The FICFB biomass gasification mentioned above is the reference of the *indirect gasification* technology, where the combustion process and the gasification process are spatially separated [Pfeifer,2004, Hofbauer,2002, Rauch,2004]. The principal of the FICFB process is shown in figure 9.

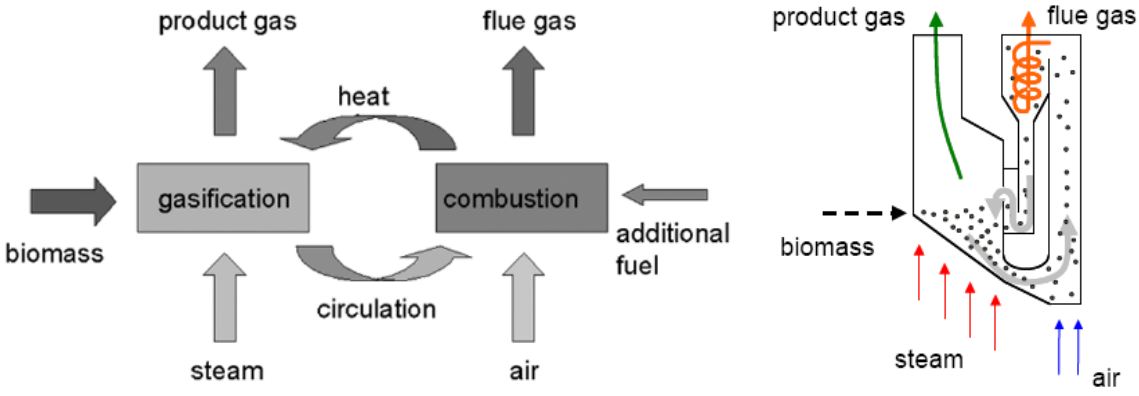

Figure 6: Principal of the FICFB gasification process realized in Guessing (Austria)

2.2. Characterization of the gas composition

Table 4 shows the gas compositions of the raw gases from the selected gasifiers after a basic cleanup (particle filter, and tar scrubber). The raw gases can be divided principally into two

groups. One group contains the raw gases with a high share of hydrocarbons, mostly in form of CH_4 and has a LHV above 3 kWh/m^3 (Bioflow, FICFB). Raw gases within the other group are a mixture of H_2/CO/CO_2 produced by entrained flow gasifiers, operating at high temperatures (GSP, Carbo-V).

In figure 10 the contribution of H_2, CO, CH_4 and C_2-species to the LHV are shown for the gasification of biomass with circulating fluidized bed, entrained flow and indirect gasification technology. The comparison shows that a major difference in the LHV results mainly from the varying content of CH_4 and C_2-species in the gas. For that reason the raw gas from the Bioflow gasifier has a much higher heating value compared to the raw gas from the GSP gasifier.

Table 2: Gas compositions of the producer gas of different gasifiers after a basic clean-up [Kirmse,2000, Eckert,1998, Rehwinkel,1990, Wolf,2001] [1)] projected gas composition for oxygen-steam-blown operation [Stahl,2005]; [2)] own measurements

		CFB[1)]	FICFB[2)]	GSP	Carbo-V
Technology		circulating	indirect	entrained flow	
H_2	[Vol.-% (LHV%)]	26.1(24.8)	41.4 (37.0)	29.0 (35.3)	40.2 (46.5)
CO	[Vol.-% (LHV%)]	16.8 (18.7)	21.5 (22.5)	45.0 (64.3)	39.3 (53.3)
CO_2	[Vol.-% (LHV%)]	35.3	20.9	18.0	20.4
CH_4	[Vol.-% (LHV%)]	12.9 (40.8)	8.2 (24.4)	0.1 (0.4)	0.06 (0.2)
C_2H_6	[Vol.-% (LHV%)]	0.2 (1.0)	0	0	0
C_2H_4	[Vol.-% (LHV%)]	2.6 (14.7)	3.0 (16.0)	0	0
N_2	[Vol.-% (LHV%)]	4.8	5.0	9.0	0.1
Tars		+	+	-	-
H/C	[-]	1.7	2.3	0.9	1.3
H_2/CO	[-]	1.55	1.92	0.64	1.02
CO_2/CO	[-]	2.10	0.95	0.40	0.52
LHV	[kWh/m^3]	3.15	3.35	2.46	2.59
HHV	[kWh/m^3]	3.48	3.71	2.62	2.81
d	[-]	0.89	0.66	0.82	0.72
Wobbe	[kWh/m^3]	4.11	4.70	2.90	3.31
Temp	[°C]	950-1000	850	1200-1400	1000
press	[bara]	20	1	25	5
Yield	[m^3/kg] η_{chG}=0.7	0.95	0.89	1.22	1.15
(water content 0.15)	η_{chG}=0.8	1.08	1.02	1.39	1.32

The evolution of CH_4 in the gasifier correlates strongly with the gasification temperature applied [Sousa,2001]. Gasification at lower temperature tends to produce methane whereas elevated temperatures do not promote the formation of methane, i.e. entrained flow gasification. Information about C_2-species is not available for all candidates, but a similar trend must be expected.

3. Efficiency estimation of SNG from biomass gasification

3.1. Experimental proof of equilibrium calculations

For the modelling in ASPEN^{PLUS} the raw gas of the FICFB gasification system is considered, as for this gasification system experimental data of methanation experiments exist. As input variable for the model the raw gas composition of the FICFB gasification system is set. Experiments at PSI proved the outlet concentrations of the methanation to be close to the chemical equilibrium (table 1). Therefore, it is possible to represent the SNG-synthesis by equilibrium calculations. This assumption is also true for the GSP gasification case, one typical entrained flow gasification technology.

Table 3: Comparison of experimental data and results of equilibrium calculations
*(H_2O added according to equation 3)

			H_2 [%]	CO [%]	CO_2 [%]	CH_4 [%]	C_2H_4 [%]	N_2 [%]
FICFB	Experiment	Input	38.4	28.9	18.3	11.6	1.1	1.3
		Output	5.2	0.3	47.7	44.1	0.0	2.7
	Chemical equilibrium		4.7	0.6	47.9	44.7	0.0	2.0
GSP	Experiment	Input	23.8	49.3	9.8	0.0	-	18.8
		Output	2.4	0.0	52.4	22.6	-	24.6
	Chemical equilibrium		2.2	0.4	51.6	22.2	-	23.6

3.2. Determination of the most promising conditions for methanation

As basis for the estimation of promising process conditions for methanation equilibrium calculations with a H_2/CO-ratio of one were carried out. For the equilibrium calculations a stoichiometric amount of water was added, according to equation 3, without considering the reaction water formed by the methanation.

$$CO + H_2 + 0.5\ H_2O \rightarrow 0.5\ CH_4 + 0.5\ H_2O + 0.5\ CO_2 \qquad (7)$$

Criteria for good process conditions are CO concentrations in the raw SNG below 0.25%. Furthermore, temperature and pressure should favour a high selectivity towards methane to maximize the CH_4-yield and minimize the H_2-concentration. In this context the CO-conversion X_{CO} (eq. 4) and the chemical efficiency of the methanation $\eta_{ch,M}$ (eq. 5) are of major interest.

$$X_{CO} = \frac{\dot{n}_{COin} - \dot{n}_{COout}}{\dot{n}_{COin}} \qquad (8)$$

$$\eta_{ch\,M} = \frac{LHV_{CH4}\ \dot{n}_{CH4out}}{LHV_{Gas\ dry\ in}\ \dot{n}_{Gas\ dry\ int}} \qquad (9)$$

The dashed square marked in figure 4b shows the area with a CO conversion higher than 99.75% which corresponds to 0.25% CO in the raw SNG. This number is essential to reach the required final CO concentration below 0.5%.

The calculations identify a suitable temperature of up to 400 °C for high pressure applications and around 300 °C for atmospheric pressure applications (figure 4). Within this area the expected CO-concentration is low enough and the efficiency is close to the maximum. The maximum achievable efficiency, however, is determined to a large extent by the composition of the producer gas.

Based on these considerations a model for the synthesis unit was set up in ASPEN^{PLUS} simulating the coupling of a synthesis unit with the FICFB gasification system. The main goal of the model is to show the feasibility of reaching the rigorous standards of the NG gas grid.

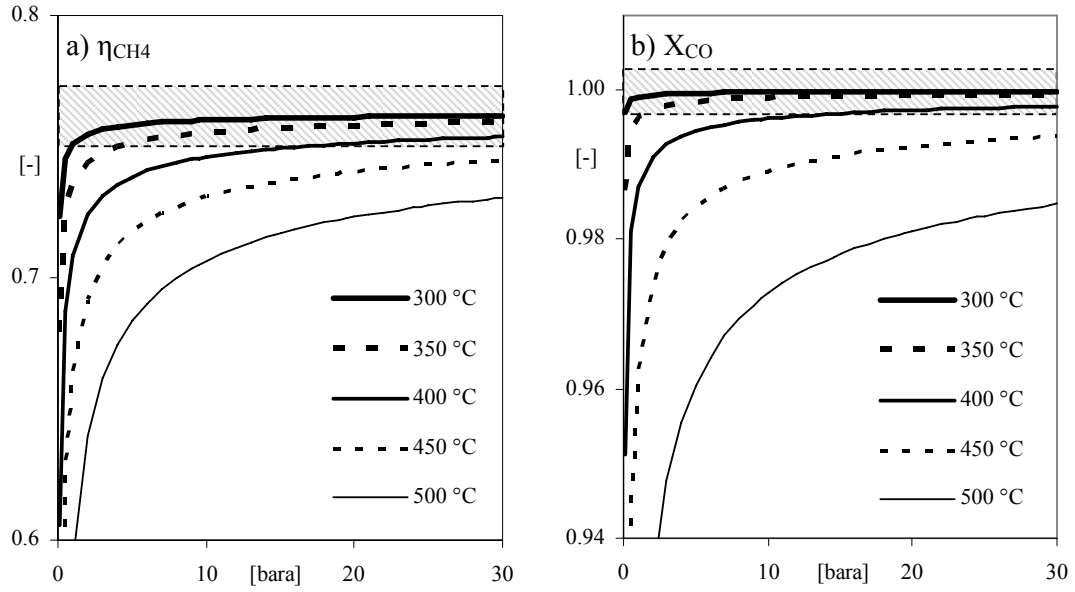

Figure 7: Identification of the most promising test conditions based on equilibrium calculations

most promising test conditions

3.3. Case FICFB

For the FICFB gasifier in Guessing, the tar load of the raw gas is reduced to about 10-20 g/m^3 of light tars by means of a RME scrubber. As inlet for the synthesis plant the gas composition of table 2 is used. In difference to table 4, the mixture contains no N_2 but a higher concentration of CO_2, simulating the exchange of N_2 used for inerting of the feeding system by CO_2.

Table 4: Results of the ASPEN^{PLUS} model for the combination of the FICFB gasifier with the SNG plant. Inlet gas composition modified such that all N2 is replaced by CO2 simulating the use of CO2 for inerting the feeding system.

		IN	OUT
H_2	[Vol-%]	41.4	2.5
CO	[Vol-%]	21.5	0.2
CO_2	[Vol-%]	25.9	2.3
CH_4	[Vol-%]	8.2	95.0
C_2H_4	[Vol-%]	3.0	0.0
HHV	[kWh/m^3]	3.35	10.60
d	[-]	0.70	0.56
S_{CH4}	[-]		0.454
X_{CO}	[-]		0.997
Pressure	[bara]	1	15
$\eta_{chem\ M}$	[-]		0.84

The fuel synthesis was modelled as an equilibrium block, minimizing Gibbs enthalpy. Chemical equilibrium calculations represent the theoretic maximum yield independent from the pathway. Under these ideal conditions there is no difference whether shift and methanation is done in separated reactors or simultaneously in a fluidized bed. Therefore, the methanation block in ASPEN^{PLUS} represents all kinds of technologies; single or multi stage methanation; separate or integrated shift. The only conditions for the validity of this assumption are that no streams are added or removed from the system and that the temperature and pressure of the last unit are equal to the conditions in the equilibrium block.

The block diagram of the modelled SNG synthesis plant is shown in figure 5. The FICFB system in Guessing is an atmospheric gasifier; therefore, the first unit in the scheme is a compressor. The gas mixture is heated up to 300 °C and a stoichiometric amount of steam is added according to equations 3 to the producer gas before it enters the methanation unit.

The parameters of the methanation are set to 320°C and 5 bara. Downstream of the catalytic reactor water is separated from the raw SNG in a condenser. After a second compression to 15 bara, the raw SNG is cleaned to natural gas quality by CO_2-separation. The split ratio for CO_2 is set to 98% relative with 2% relative loss of CH_4 simulating a pressure swing adsorption (PSA) [Ramesohl,2005]. The profile of temperature and pressure along the process path is shown in figure 6.

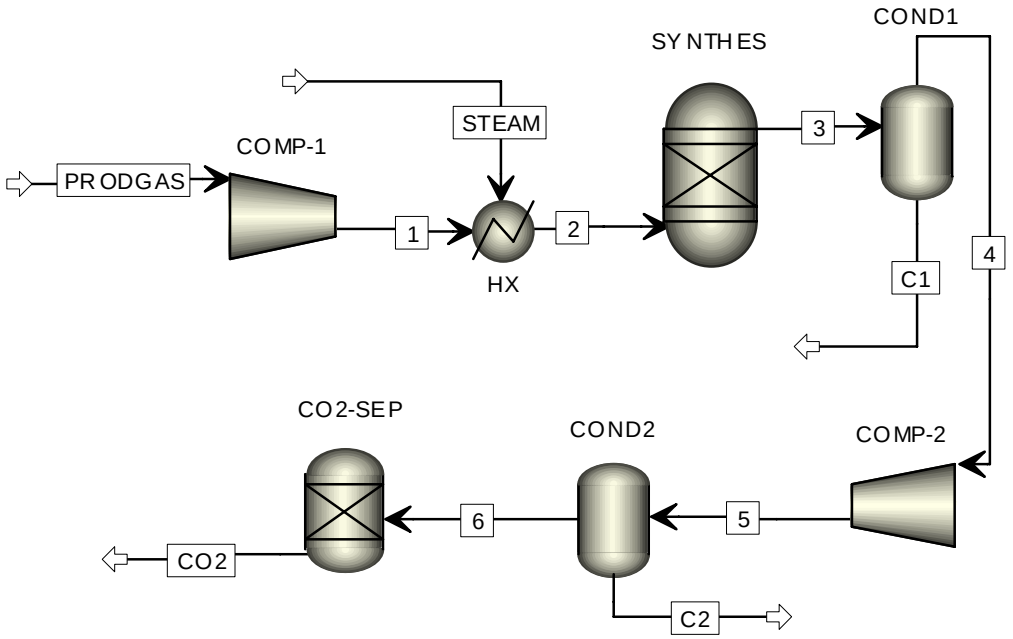

Figure 8: Block diagram of the ASPEN^{PLUS} model and characteristic of temperature and pressure

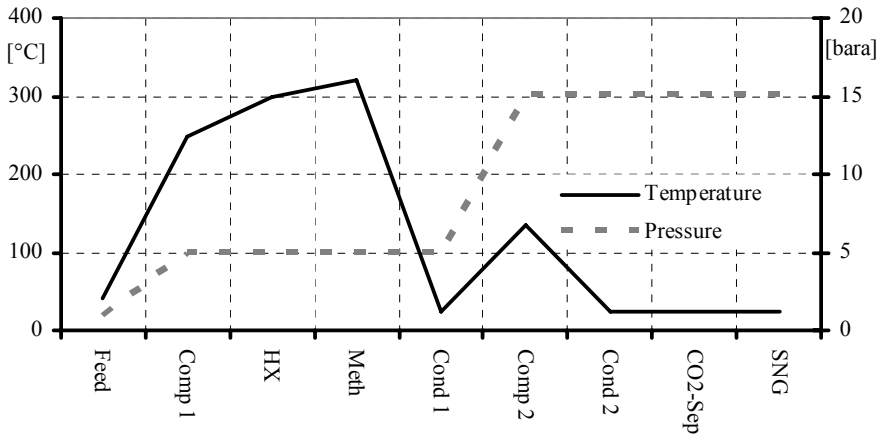

Figure 9: Characteristic of temperature and pressure of the ASPEN^{PLUS} model

3.4. Results

The composition of the SNG according to the model is shown in table 2. The chemical efficiency of the synthesis is 84%. This value corresponds well with the efficiency demonstrated experimentally on site of the FICFB gasifier in 2003 [Seemann,2005] (83%). A published value for the efficiency of the FICFB gasifier is 76% [T.Proell,2004]. Therefore, the optimistic overall chemical efficiency is calculated to be 64%. The produced steam and the used power for compression are not considered in this efficiency number. The concentration of CO of 0.2% is within the margins discussed for the injection into the NG grid.

In figure 2 the HHV of dry gas mixtures is plotted versus the relative density. Both parameters

are relevant numbers for the characterization of NG qualities. The quality requirements for SNG according to the G 260 are marked by the hexagonal area in the upper part of the diagram. The premium gas quality (H-gas) valid for wide parts of the
German NG grid is in the upper part of this hexagon. The producer gases from coal and biomass are located around 3 kWh/m^3. The changes of the gas mixture due to the different operation units of the synthesis plant are indicted by arrows. 1-2 is the fluidized bed methanation featuring integrated shift. Alternatively a shift step to 1b is possible to apply fixed bed methanation (1b-2). The CO_2-separation from 2-3 increases the HHV of the gas mixture and lowers the relative density.
The final composition of the SNG from the model fulfils the requirements of H-gas quality according to the rules of the DVGW. In case the HHV of the gas after the CO_2 separation is still too low, further upgrading of the gas by H_2-separation is possible.

The FICFB system is a special case; as the CO_2 produced by the partial combustion of feed for the autothermal heat production is released separately. Therefore, the producer gas has a high LHV, even though it contains much less CH_4 and C_2-species than the Bioflow.

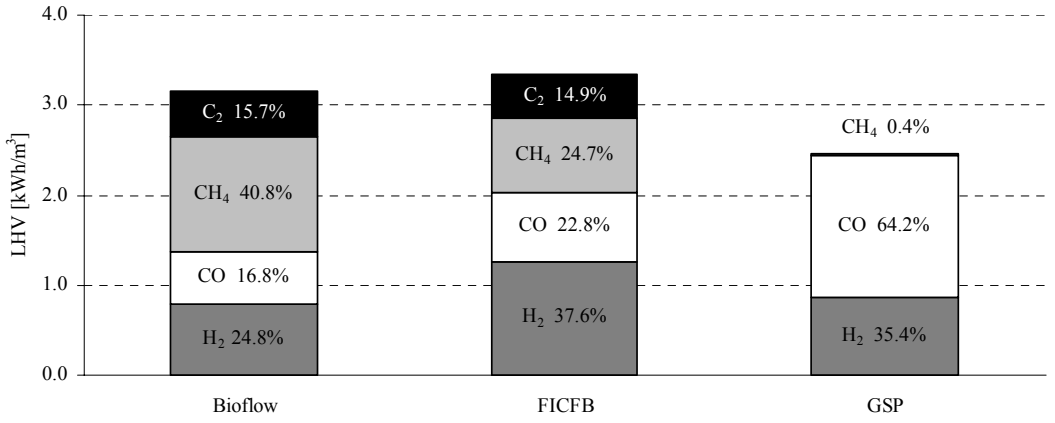

Figure 10: Contribution of the H_2, CO, CH_4 and C_2 species to the LHV of the raw gas of different gasification technologies: circulating fluidized bed, CFB; indirect gasification, FICFB; Entrained flow GSP.

3.5. Producer gas composition and overall chemical efficiency

The chemical efficiency, $\eta_{ch\,M}$ (eq. 10), of the catalytic conversion is determined by the reaction enthalpies, ΔH_R of the methanation and the WGS reaction. For the methanation, ΔH_R is -206 kJ/mol and for the WGS reaction -41.1 kJ/mol; corresponding to a chemical efficiency of 79.5% and 85.5% respectively.

$$\eta_{ch\,M} = \frac{LHV_{CH4}\ \dot{n}_{CH4out}}{LHV_{Gas\ dry\ in}\ \dot{n}_{Gas\ dry\ int}} \qquad (10)$$

Obviously, the chemical efficiency of the conversion of producer gas to SNG depends mainly on the amount and the ratio of H_2 and CO in the mixture. The higher the share of H_2 and CO in the gas the lower is the chemical efficiency of the synthesis. As a matter of fact, the thermal losses of the catalytic step are determined by the gasification system and the chemical efficiency numbers of the fuel synthesis must be rated in this context.

In table 5 the maximum stoichiometric output and the maximum chemical efficiency of a synthesis unit are calculated for each of the gas compositions, based on stoichiometry. The concentrations of CH_4 in the raw SNG and the chemical efficiency of the producer gases of the group of gasifiers, containing already hydrocarbons, are significantly higher (table 4).

Table 5: Maximum output of the methanation for different raw gases according to stoichiometry, the chemical efficiency of the gasification is assumed to be between 70 and 80%

		CFB	FICFB	GSP	Carbo-V
CO_2	[Vol.-%]	56.82	44.52	61.72	66.53
CH_4	[Vol.-%]	36.80	47.36	25.80	33.29
N_2	[Vol.-%]	6.39	8.12	12.48	0.18
LHV	[kWh/m^3]	3.76	4.72	2.57	3.32
HHV	[kWh/m^3]	4.18	5.24	2.85	3.68
η_{chM}	[-]	0.876	0.879	0.745	0.766
η_{ch}	(η_{chG}=0.7)	0.61	0.61	0.52	0.54
	(η_{chG}=0.8)	0.70	0.70	0.60	0.61

To asses the influence of the producer gas composition on the overall efficiency the conversion from wood to SNG is calculated once for the GSP gasifier (case I) yielding an almost pure H_2/CO mixture and once for the Bioflow gasifier (case II), yielding a raw gas containing H_2, CO, CO_2, CH_4 and C_2H_4. For the calculations a chemical efficiency of 80 % for the gasification system and stoichiometric conversion in the shift and the methanation unit are assumed; C_2 species in the producer gas are converted to CH_4. In table 6 the conditions and the results are shown for both cases.

The chemical efficiency for the Bioflow with 70 % is significantly higher than for case I the GSP with 60.4 %. The reason for this difference is the release of reaction heat from methanation and WGS reaction during the fuel synthesis. Therefore the loss of chemical energy in the synthesis unit is linked to the amounts of CO and H_2 in the raw gas. In case of the Bioflow gasifier a part of this reaction heat is “integrated” into the gasification process. Therefore, raw gases with a high share of CH_4 are favourable for the SNG production as the overall chemical efficiency is increased.

Another important issue is the amount of inert gases in the raw gas. The concentration of inert

gases multiplies as the overall volume of the gas is shrinking due to the methanation reaction and the subsequent CO_2-separation. As the content of CH_4 has to be in the region of about 95 % to reach the required HHV the content of inerts in the producer gas needs to be 0.5 %. All presented gasification technologies need to take further measures to reduce the nitrogen content to be compatible with the requirements for SNG production. The main source of the inert gas is the feeding system, which is usually pressurized with nitrogen. To avoid N_2 in the producer gas, pressurization could be done with CO_2 instead.

Table 6: Comparison of the gas composition of GSP and Bioflow gasification technology according to their stoichiometric yield of SNG

	GSP (case I)		Bioflow (case II)
Assumptions	0.8	Cold gas Efficiency of Gasifier	0.8
	$H_2/CO=0.64$	Gas compositions	$H_2/CO=1.55$
	no CH_4 and C_2H_x		with CH_4 and C_2H_x
		Losses	
	100 %	Gasification	100 %
	80 %	Shift	80 %
	75.6%	Methanation	79.1 %
	60.4 %		70.0 %

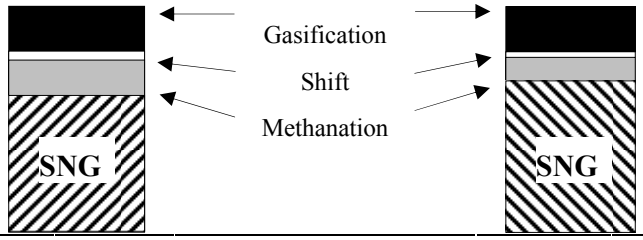

II. Proof of concept for gaseous fuel production, using a slip stream of the FICFB gasifier in Güssing

1. Introduction

The aim of the task 5.5.3 is to supply consistent data from long term testing, using a slipstream of the FICFB gasification power plant in Güssing. Next to the experimental proof of concept for the fluidised bed methanation process on pilot scale, quantitative targets for the necessary gas cleaning should be determined.

For proving the concept of SNG production from FICFB gasifier producer gas under real conditions, the mobile container-based system for methanation (COSYMA) was set up. This new 10 kW reactor system is designed for unattended operation at conditions between 1.2 and 10 bars and 300 - 500°C. At these conditions, synthetic experiments with gas mixtures from bottles as well as (long term) on-site experiments with producer gas from a gasification system were possible.

The design and construction of COSYMA are described in chapter 2; the following section describes the first tests and experiments carried out at PSI. In chapter 4, the first two long duration tests at Güssing in 2004 are presented, whereas in section 5 the results of these experiments are discussed. In Chapter 6, the most important analyses of catalyst samples and the subsequent conclusions concerning the further research on possible deactivation mechanisms are shown. Chapter 7 describes the experimental work at PSI on understanding the role of carbon atoms on the catalyst surface, being necessary intermediate as well as potential catalyst poison. The following section 8 focuses the successful experimental effort in Güssing to improve the gas cleaning by introduction of a hydrodesulphurization step (HDS). Chapter 9 contains the conclusions concerning the proof of concept and necessary quality of the gas cleaning system.

Results of previous work

The main goal of the first experimental campaign in Güssing (Austria) in 2003, financed by the Swiss Federal Office of Energy (BfE), was the proof of concept for the production of SNG via a combination of biomass gasification with a methanation unit. The hypothesis was developed, that shift, methanation, and reforming reactions can take place simultaneously in a single fluidized bed and, therefore, neither an additional shift unit nor a reforming unit is needed.

For this purpose, a 2 kW fluidized bed reactor (COALA) was put into operation at PSI in 2002. Several catalysts were tested with model syngas compositions (pure gases, mixed by mass flow controllers). After identifying a promising catalyst, the campaign with producer gas derived from biomass was planed on site of the FICFB (Fast Internally Circulating Fluidized Bed) gasification system in Guessing. Objective of the campaign was the testing of the catalyst under the harsh conditions of a producer gas and the generation of data for a scale up of the concept.

In May 2003, producer gas from a biomass gasification system was converted to SNG on lab scale for the first time (world wide).

To characterize the performance of the catalytic process, the following key figures were used:

CO-conversion X_{CO}

$$X_{CO} = \frac{n_{COin} - n_{COout}}{n_{COin}} \quad (1)$$

The conversion of light tars X_{BTN}; where BTN is an abbreviation for the main compounds of light tars benzene, toluene and naphthalene.

$$X_{BTN} = \frac{n_{BTNin} - n_{BTNout}}{n_{BTNin}} \quad (2)$$

The chemical efficiency η_{ch} shows the conversion efficiency of the energy content.

$$\eta_{ch} = \frac{LHV_{Methane\ out} \quad \dot{m}_{Methane\ out}}{LHV_{Gas\ dry,\ tar\ free\ in} \quad \dot{m}_{Gas\ dry\ in}} \quad (3)$$

It is important to mention that the tars are not considered in the LHV (Lower Heating Value) as they can normally not be converted to a useful product in catalytic processes such as Fischer-Tropsch-Synthesis.

The catalyst proved its promising results from the pre experimental tests:
- High activity and selectivity, resulting in a CO conversion X_{CO} of more than 98% and a chemical efficiency η_{ch} of almost 85%.
- High tolerance towards contaminants; ammonia and light tars
- Good mechanical stability; the total weight loss during the 120 hour experiment was only 6 wt %. This value combines from 4.6 wt % of fines in the raw catalyst, which are carried out with the first moments of fluidization and 1.5 wt % due to attrition. Due to the positive features of the catalyst, the hypothesis of simultaneous shift, methanation, and tar reforming could be validated. With the operation conditions chosen, the tars are even considered as energy and carbon source for the SNG production. Despite the contamination of the producer gas with ammonia and unsaturated hydrocarbons the catalytic activity was stable during 120 hours.

The experimental campaign also exposed some weaknesses of the experimental setup. Condensation of water and naphthalene from the producer gas caused manifold problems in the unheated parts upstream of the methanation reactor. The aqueous condensate had to be removed frequently from low lying parts of the tubing. The naphthalene, in contrast, crystallized and formed a coating of 1 2 mm inside the tubes. Hence the pressure resistance increased during the experiment, the gas flow decreased steadily. Therefore, the gas pump overheated and shut down.

For further long term experiments, following improvements were found to be necessary:
- Adequate and reliable gas pump
- Heated tubing upstream of the methanation unit to prevent condensation
- Tempered gas meter, with pressure and temperature measurement at inlet and outlet of the methanation setup
- Control unit for unattended operation

2. Design and Construction of COSYMA

For proving the concept of SNG production from FICFB gasifier producer gas in long-term experiments under real conditions, the mobile container-based system for methanation (COSYMA) was set up. As the name implies, COSYMA is mounted in a 20 foot container. The inventory of the container is structured in three main parts; the methanation unit, the control unit and the analytics. As shown in figure 1, the three modules of the system are placed along the back wall of the container. For safety reasons, this area is ventilated extremely well and is separated by Perspex panels from the work space of the operating staff. Along the other wall a workbench is placed underneath of the windows, carrying the two computers needed for operating of the set-up.

Figure 1 COSYMA at the site of the FICFB gasification system in Güssing; floor plan of the container

2.1 Methanation unit

As shown in the process and flow diagram of the methanation unit, there are two alternatives for the gas supply (figure 2). For synthetic experiments, the gas is mixed from bottles via a six mass flow controllers (H_2, CO, CO_2, CH_4, C_2H_4, and N_2) and for experiments on-site a frequency controlled compressor can transport the producer gas into the reactor system.

To prevent condensation, the tubing is heated along the complete distance between the gasification system and the methanation set-up. The gas is sucked through a tempered (50°C) box. Inside this box, the producer gas is led through a custom gas meter, counting the total gas volume. By combination with temperature and pressure measurement, the calculation of the average flow is possible. For the determination of real time variations of the flow, additionally an orifice plate with two pressure transducers is placed in this box.

The gas is compressed and led through two heated fixed bed reactors filled with ZnO for the adsorption of H_2S. After the desulphurization units, the producer gas is conditioned with water

and, optionally for synthetic experiments, with tars. The water is fed by a high precision piston pump from a 60 l reservoir into the evaporator.

Core of the setup is a fluidized bed reactor of similar dimensions as the lab reactor COALA. The reactor of about 50mm diameter ends in a diffuser to control the discharge of fines. The gas is introduced through a porous glass plate. Axially, five staged thermocouples are introduced from the top of the reactor to measure the temperature distribution along the bed. The temperature in the reaction zone is controlled by cooling the outside reactor wall with air from a blower. For heating up the system, and to perform endothermic reactions, the air can be heated up to 500°C by a 3 kW electrical heater, installed in the air path.

Gas leaving the reactor passes a candle filter (5 µm) for particle removal and two condensers to remove the produced water from the raw SNG. The first of the two condensers is air cooled and the second one is cooled with a refrigerant from a closed cycle cooling system. The condensate is collected in a 6 l container positioned on a balance. When the balance reaches its limit, the vessel is emptied by a pump into a barrel.

At the end of the system is the pressure valve for the range between 1.3 and 10 bars and another gas meter for the measuring the dry gas volume leaving the reactor system.

In the reactor system, three mechanical safety valves, opening above 10bar, are mounted at sensible positions.

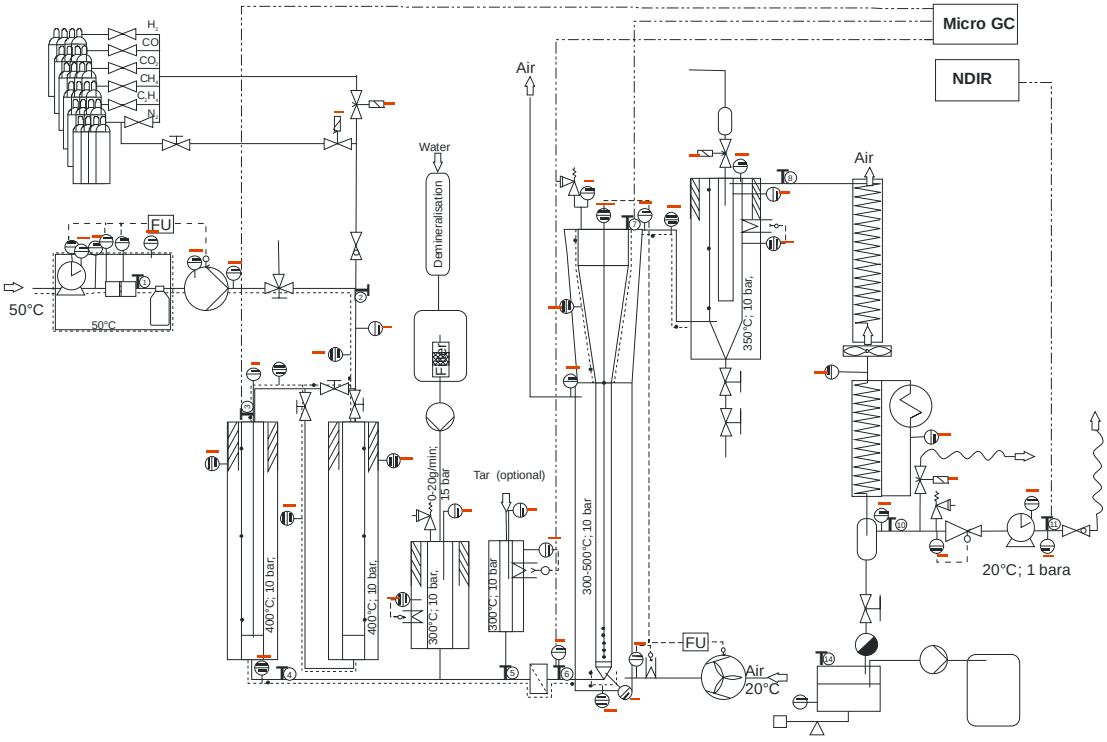

Figure 2: Process and flow diagram of the methanation test rig (scale1:400)

2.2 Analytics

For the main process control, the dry gas stream behind the pressure containing valve is analyzed permanently by means of a non dispersive infrared detector (NDIR). This detector

analyzes the three main carbon containing species; CH_4, CO_2 and CO.
The methanation set-up is equipped with totally eleven sampling points between each of the main operation units; the first one in the heated inlet box and the last one after the outlet gas meter. At these sampling points, the full range of gaseous compounds can be analyzed by a 2x2 µ-GC (Varian CP-4900; TCD detector). This µ-GC contains two sampling paths with two columns each (Columns; MSA5, PPU). One column is for the measurement of H_2, N_2, CO, CH_4 and the other one for CO_2, the C_2 and C_3 species. With this combination, simultaneous measurements upstream and downstream of an operation unit are possible. To protect the GC against condensable hydrocarbons and water, an advanced liquid quench system is applied. The cleaning solvent in the liquid quench system is also used for post experimental GC-MS analysis of the condensable compounds of the gas.
As described above, the measurement of the gas flow is improved by accompanying the gas meters with temperature and pressure measurement and by placing the one at the inlet of the methanation system in a heated box. Additional, pressure transponders are placed upstream and downstream of the main operation units to monitor the pressure drop through the plant. Furthermore, the temperature is measured at each operation unit and in the gas stream all over the system.
In the campaign 2003, catalyst samples could only be taken when the reactor was cooled down. Therefore, a **u**tility **f**or **o**xygen-free sampling (UFO) was constructed. With this utility, catalyst samples from the hot reactor during reaction can be taken. The samples are removed from the UFO in little glass containers with a polyethylene cover without contact to air.

2.3 Control unit

For unmanned long term experiments, a control unit was set up to keep the system within the target conditions and avoid undesired states of the plant. Several internal and external safety and operation issues like leakage, blockage or a shut down of the gasification system are considered in the design. Depending on the situation, the unit sets the reactor system into stand-by mode or shuts it down. The program is monitoring temperature, pressure, status of the gasification system, and the gas sensors in the container. For the safety of the operating staff, sensors for CO, CH_4 and H_2 concentration in the air are placed in the container. Via a special port, the control unit can be manipulated from outside of the container via internet access from PSI. To keep control even in severe conditions the power supply is secured by an independent accumulator unit.
If any of the limit values is exceeded, the methanation set-up is shut down immediately. This means, stopping of all inlet streams, opening of the pressure containing valve and flushing of the system with N_2. If necessary, the temperature of all compounds is lowered to room temperature. In case of minor problems, like a shut down of the gasification system, the methanation unit is heated externally to enable a restart.

Figure 3: View into the container on the control unit and the methanation system

3. First tests and experiments at PSI

Before experiments could be started on COSYMA, several tests were performed to secure the functionality and safety of the setup. These basic tests included a leak test with helium, heating and/or cooling of all operation units and functionality test of the control unit. Furthermore, each operation unit was tested with respect to its eventual reactivity with synthetic gas mixtures (blank test), before a small charge of catalyst was filled into the fluidized bed. With simple H_2/CO mixtures, the limits of the cooling system of the methanation reactor were tested. After finishing the tests successfully, first experiments were started with COSYMA.

3.1 Variation of temperature and pressure

The first experiment was thought to determine the optimum reaction conditions for the composition of the producer gas from the FICFB gasification system. Following the gas compositions found by the μ-GC and GC-MS measurements in 2003, the gas mixture was mixed from bottles and optionally, 15 g/m^3 of a BTN mixture were added. The conversion of tar loaded and tar free gas mixtures was studied in the range between 350°C and 450°C and between one and five bar. As predicted by the chemical equilibrium calculations, the gas composition at the outlet responded on the variation with higher conversion at low temperature and high pressures. In general, the methane contents in the raw SNG varied between 40 and 45%. As already observed in the Güssing campaign 2003, the presence of tars in the gas mixture influenced the methane selectivity positively.

3.2 Long duration test at PSI

As preparation for the field campaign in Güssing, a long duration test with a synthetic gas mixture was performed at operation conditions identified in the variation experiments described above. The catalyst was treated over 100 hours with the gas composition similar to the one measured in Güssing 2003, loaded with 15 mg/m^3 of a synthetic tar mixture. As visible in figure 4, the CO-conversion and the CH_4 concentration in the outlet was constantly high. Apart from slight changes, mainly caused by varying water and tar supply, the performance of the catalyst was stable. The identified operation conditions appeared to be sustainable and the catalyst performance was stable over almost 100 hours.

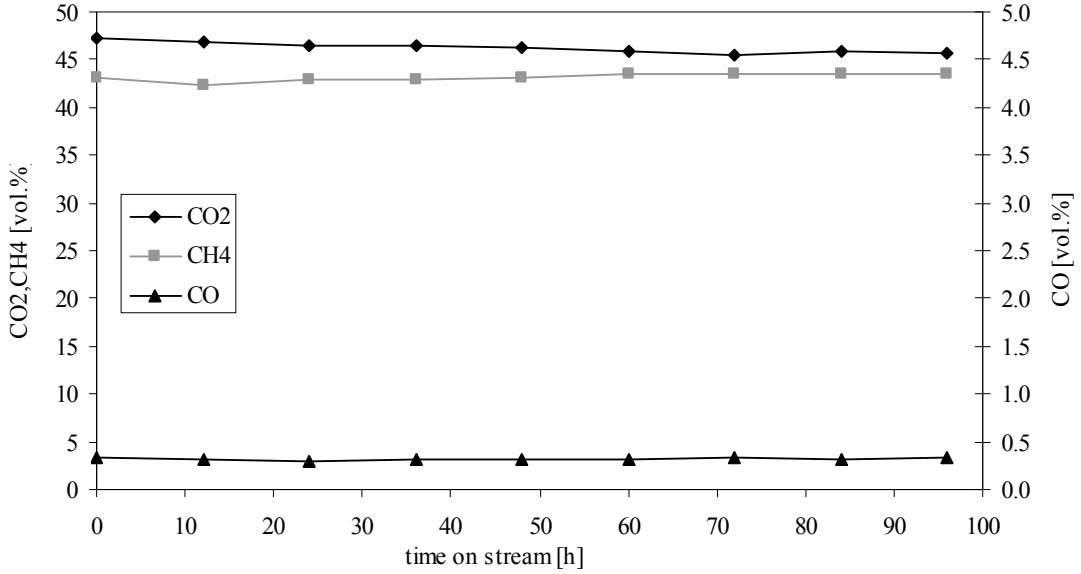

Figure 4: Concentrations of CH_4, CO_2 and CO measured by NDIR. Feed is a synthetic gas mixture simulating the composition of producer gas from the FICFB gasification system

3.3 Experimental simulation of a two-stage methanation

The limit values of CO in the SNG for the injection into the natural gas grid are not published yet, but expected to be quite strict. To assess the lowest concentration of CO reachable in a bubbling fluidized bed with the applied catalyst, a two stage concept was simulated. For the simulation, the results form the long-term experiment described above were used as reference for the first stage. Consequently, the values of the outlet gas composition from the long term experiment were applied as inlet gas composition for the second stage. Table 1.1 shows the gas compositions at the inlet and outlet of the long-term experiment in the first columns.

By simulating several measures like CO_2 removal, addition of steam, operation conditions for a second stage were evaluated.

No major decrease in CO-concentration was achieved before the CO_2 was removed from the gas-mixture (table 1, column 3). This measure would simulate a CO_2-removal by pressure swing adsorption (PSA) or an amine scrubbing before the 2nd stage. To sustain good fluidization the missing gas volume had to be replaced. This was done with N_2 as the mass-

flow-controller of CH_4 did not have the potential. The gas was fed without water into the reactor at the level of 10 bars as in a real process; the gas has to be dried before compression. At conditions of 300°C and 10 bars with simulated CO_2-removal, the CO-concentration decreased below 0.1 vol % (table 1).

Table 1: Gas composition at the inlet and outlet of the methanation reactor during the simulation of a two-stage methanation unit, the outlet of the simulated second stage was only measured by means of a NDIR. (*CO_2 is replaced by additional N_2

Species	1st Stage (96h long-term)		2nd Stage (optimum result)	
[mol%]	IN (µ-GC)	OUT (µ-GC)	IN (µ-GC) (*	OUT (NDIR)
H_2	36.9	4.1	4.9	
CO	25.3	0.4	0.5	< 0.1
CO_2	18.2	47.4	0.0	1.2
CH_4	9.7	39.6	39.2	42.1
C_2H_2	0.0	0.0		
C_2H_4	0.0	0.0		
C_2H_6	3.1	0.0		
N_2	5.9	8.4	55.6	
Total	100	100	100	

4. First long duration tests in Güssing 2004

After the successful synthetic experiments at promising test conditions, the container COSYMA was shipped to Güssing and placed on the site of the FICFB gasifier (figure 5). A heated gas pipeline (60°C) was constructed, leading producer gas from the gasifier to the methanation system. The turn-off for the split stream to COSYMA is between product gas scrubber and the gas engine. Consequently, the gas going into the methanation reactor is of the same quality as for the gas engine. In figure 6, the process and flow diagram of the FICFB gasification system is shown.

Connected to internet and power supply, the setup was ready for first tests. COSYMA was set into operation with catalyst already used during the previous experiments. The gas supply with producer gas was tested and the settings for the operation of the compressor were identified. With the COSYMA running stable, emergency, stand by and shut down scenarios were tested.

Figure 5: COSYMA on the site of the biomass CHP plant in Guessing

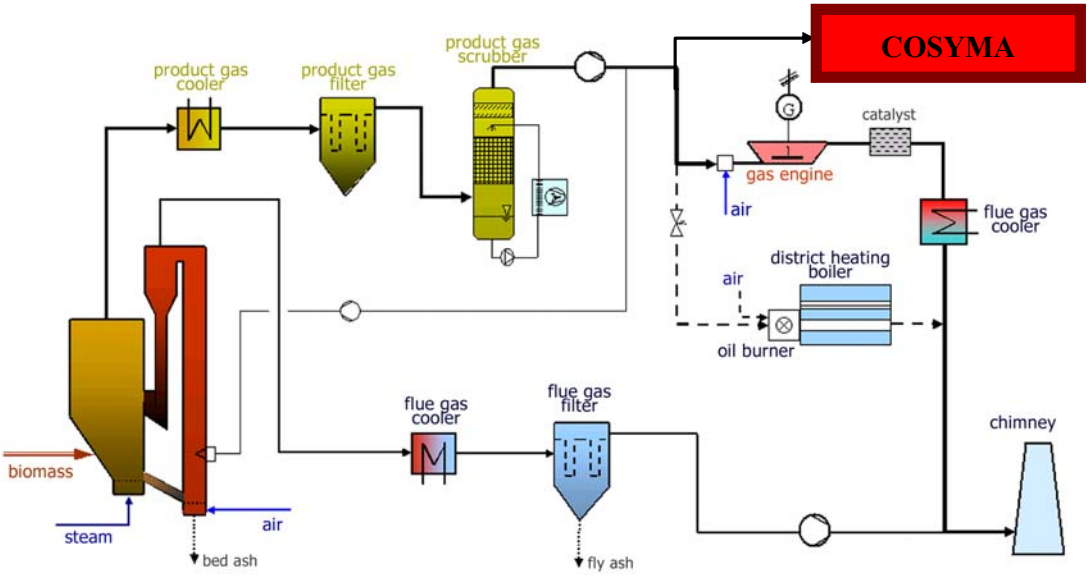

Figure 6: Process and flow diagram of the CHP plant in Guessing

4.1 Experiment COSYMA_3 (October 2004)

Based on the experiences of the preliminary tests with COSYMA at PSI, a first long duration test was started in October 2004. A new charge of catalyst was filled in the reactor and the catalyst was treated for one hour with a $H_2/CO=3$ mixture. Afterwards, the compressor was started. The operation conditions of that experiment were similar to the 100 hours of trouble free operation in the experiment with synthetic gas mixture.

For most of the time, the concentrations of CH_4, CO_2 and CO at the outlet of the system (see figure 7) were similar to that obtained in the synthetic experiments shown in figure 4. The fluctuations are mainly evoked by fluctuations of the producer gas composition or flow, respectively.

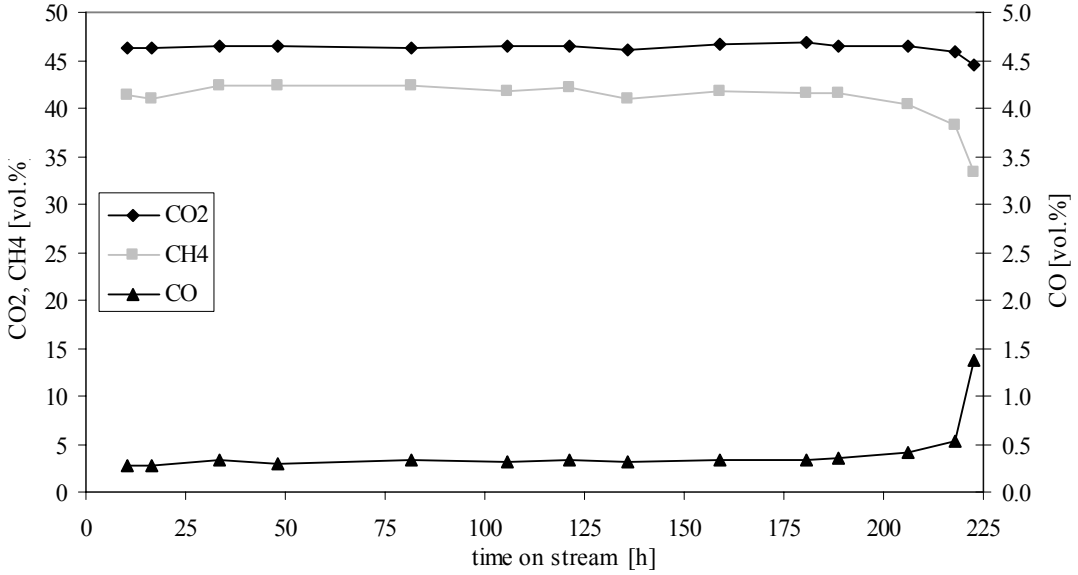

Figure 7: Average concentration in the raw SNG measured by NDIR, during the experiment COSYMA_3

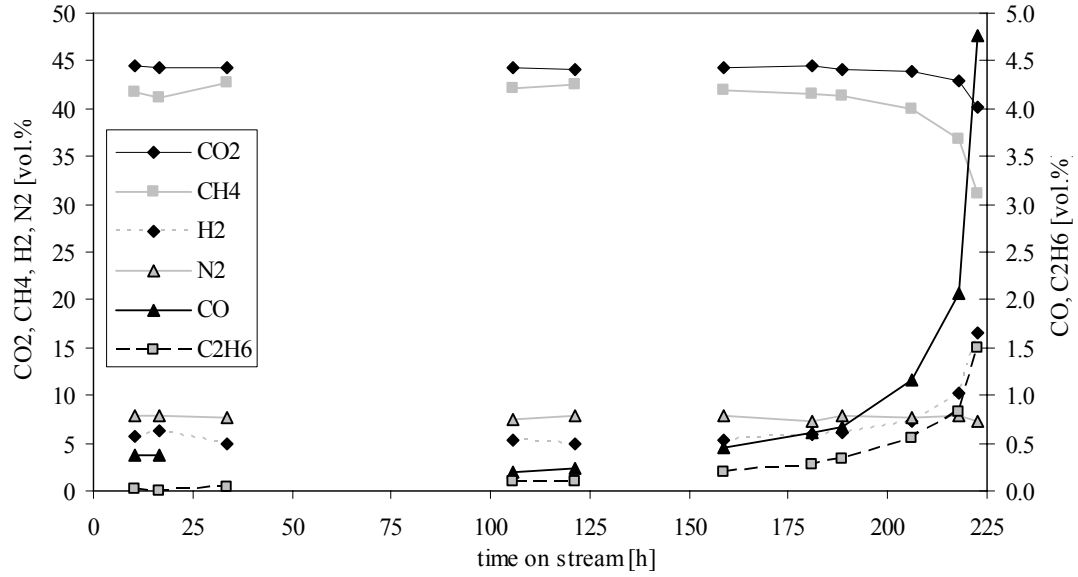

Figure 8: Average concentration in the raw SNG measured by µ-GC, during the experiment COSYMA_3

After 140 hours on stream, the water supply broke down and the reaction ran "dry" for about 10 hours. Due to massive carbon deposition, the activity of the catalyst decayed and the reactions started to die out. By steaming of the catalyst for several hours, the carbon could be removed, and the reaction was restarted. As the graphs of figure 7 display only average values for the

time on stream, this incident is barely visible on this chart.
The long-term experiment COSYMA_03 lasted for about 230 hours until the catalyst deactivated definitely. Similar to the experiment 2003 with the extended COALA setup, the increasing amount of C_2H_6 in the raw SNG was the only evidence for the decay of the catalyst. The increase of C_2H_6 was slow in the beginning and accelerated with time until the methanation reaction died out (Figure 8).
This final decay of activity was assumed to be caused by a break through of H_2S as the amount of used sulphur adsorbent (ZnO) was low. Whereas the catalyst could be regenerated from the coking after 140 hours, the poisoning with sulphur diminished the activity of the catalyst irreversibly and ended the experiment. The result of 1-2 wt% sulphur in the post-test analysis of the catalyst by X-ray Photoelectron Spectroscopy (XPS) supported the assumption about a sulphur breakthrough as reason for the deactivation.

4.2 Experiment COSYMA_4 (November 2004)

For the start of experiment COSYMA_4, additional sulphur adsorbent was placed in the two desulphurization units. All other operation conditions were the same. Compared to the experiment 3, the experiment was interrupted several times by technical shut downs of the gasification system. The technical difficulties with the gasification system resulted in an unsteadiness of the producer gas composition, effecting the composition of the raw SNG as well (figures 9 and 10). However, the multiple interruptions proved the robustness of the control unit and the methanation setup.
Even though the amount of ZnO was increased, the catalyst deactivated again after 200 hours. Both, the signal of the NDIR as well as the results of the μ-GC analysis, show the same characteristic as found in experiment COSYMA_3.
The post-test analysis showed again a significant amount of sulphur in the catalyst (1-2 wt%). Since the amount of ZnO was sufficient for the H_2S removal, the sulphur poisoning was most probably evoked by organic sulphur species.

4.3 Experiment COSYMA_16 (Spring 2007)

Within the European Union project BioSNG, several further long duration tests were carried out to investigate the influence of different operation parameters. The last test was started in April 2007 and ran until the summer revision break of the gasifier. As sulphur poisoning was one of the main issues during previous tests, special attention was paid to optimise the sulphur removal. As can be seen from figure 11, the sulphur deposition rate was slow enough to enable catalyst stability for more than 1000 hours with a high methane content of about 40% and very little CO amount (smaller than 0.5%).

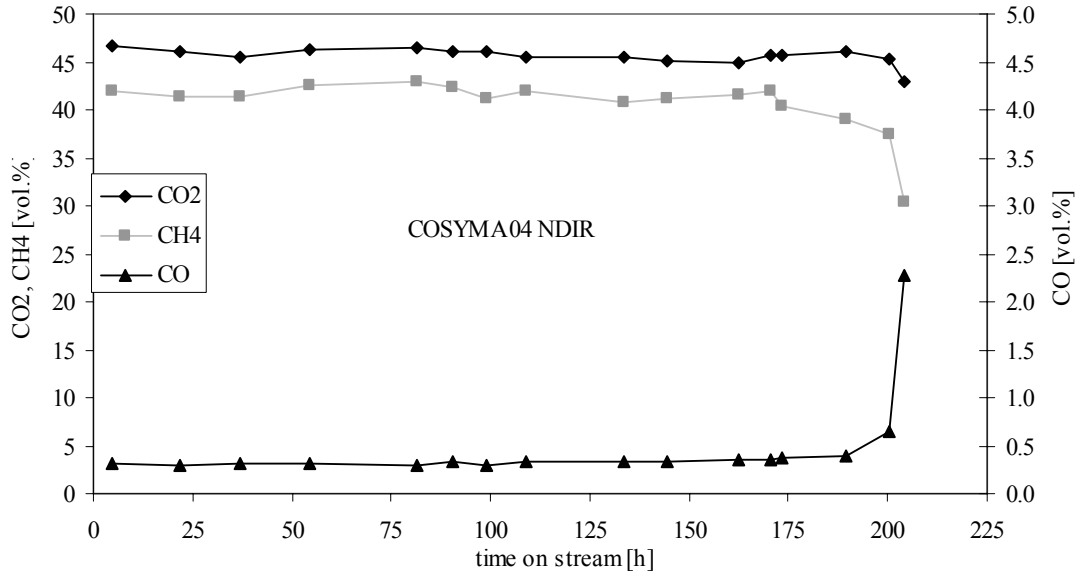

Figure 9 Average concentration in the raw SNG measured by NDIR, during the experiment COSYMA 4

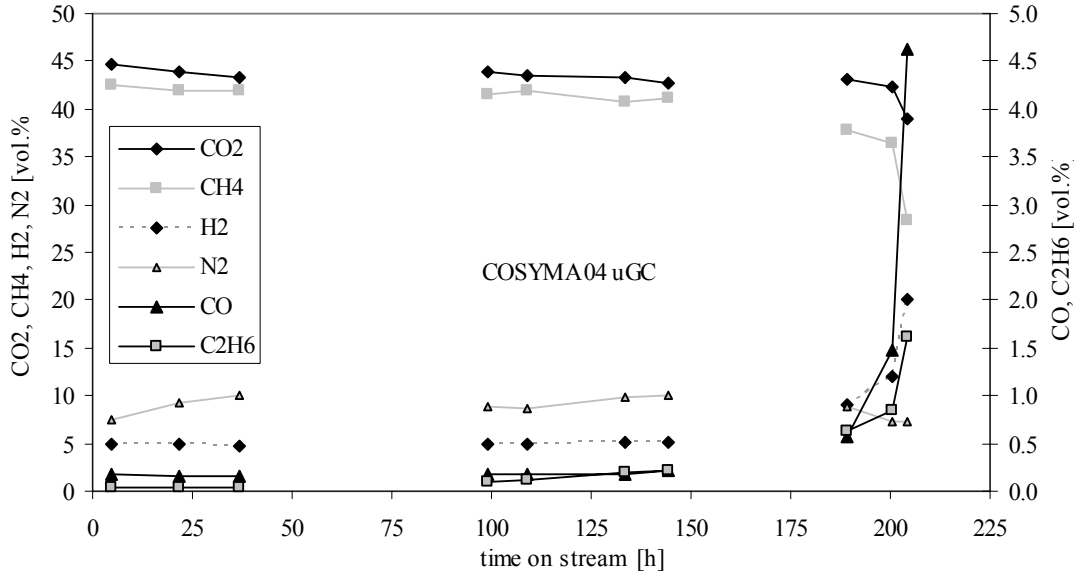

Figure 10 Average concentration in the raw SNG measured by μ-GC, during the experiment COSYMA_4

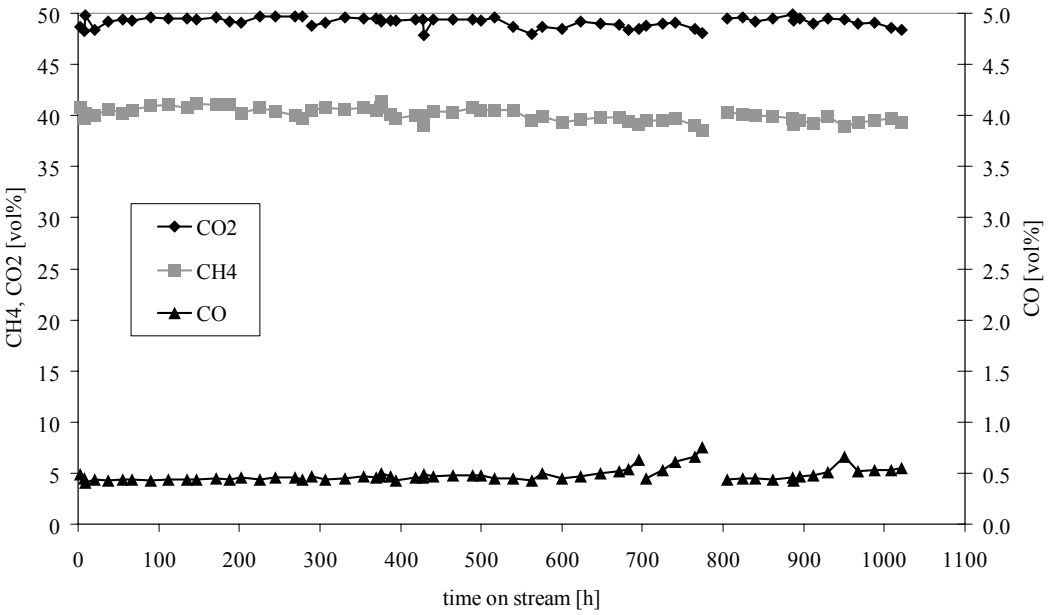

Figure 11 Average concentration in the raw SNG measured by NDIR, during the experiment COSYMA 16

5. Conclusions of the slip stream testing

In the first experiments, the set-up proved its robustness. The control unit met the demands for operator convenience and safety. The monitoring and control of the setup during the periods of unmanned operation via internet proved to be a valuable tool. Compared to the campaign in 2003, the quality of the analytics was improved, so that the atomic balances are closed to 98% now. Already during the test period, valuable results for further ASPEN calculations were obtained. As a matter of fact, no general changes of the setup are needed.

However, the resume of the first long duration test was less positive. Even though the results from 2003 were reproduced in Cosyma_3 and _4, the goal of 1000 hours of operation was not reached in the first attempt. But finally with an improved sulphur removal system it could be shown, that a catalyst could be run on stream over more than 1000 hours.

Although a break-through of organic sulphur compounds was assumed to be the reason for the decay of the catalytic activity, all possible deactivation mechanisms were taken into account, such as sintering of crystallites, changes in the catalyst support, poisoning, removal of the active phase from the reactor and deposits blocking the access to the catalytic sites.

6. Detailed post-test analyses of catalyst samples

For the investigation of the deactivation mechanism, detailed analyses of the catalyst samples were carried out.

6.1 Temperature Programmed Oxidation

With this method, a catalyst sample is heated under a flow of an oxygen/argon mixture while a microbalance records the change in mass of the catalyst sample. The gas flow leaving the sample chamber is analyzed by an infrared spectrometer. Figure 12 shows a typical result of such an analysis. The red curve gives the temperature measured at the sample while the blue curve shows the relative change in weight. It can be observed that after drying of the sample in the first ten minutes, an exothermic reaction takes place at about 250°C, accompanied by an increase in sample mass. The evolution of the CO_2 (green curve) shows a narrow peak at the same moment. While this CO_2-peak can be assigned to the combustion of adsorbed tars, the increase in weight can only be explained with the complete oxidation of bulk metallic nickel.

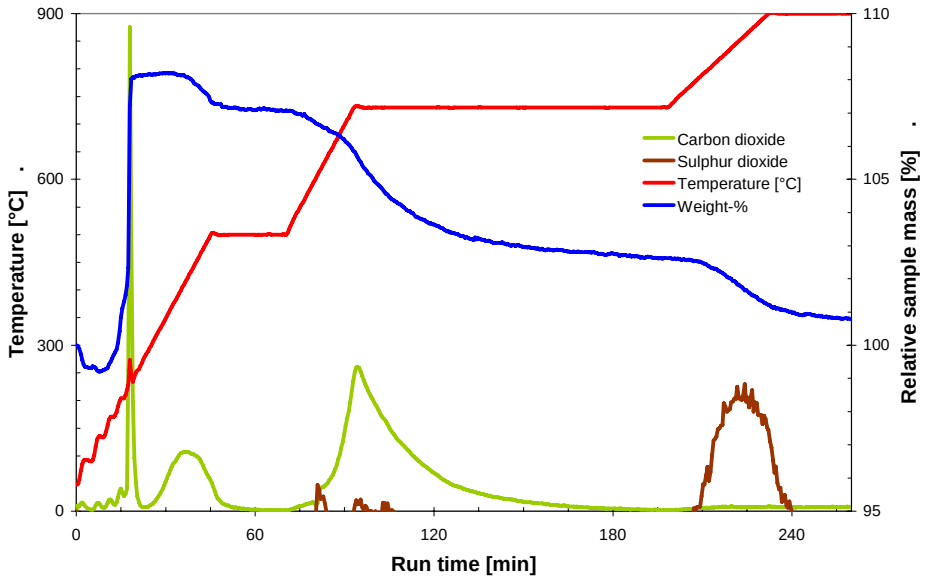

Figure 12 TPO of Ni/γ-Al_2O_3 catalyst deactivated during methanation experiments with product gas from the industrial biomass gasifier in Güssing/Austria

In the further progress of the analysis, the weight curve only shows losses indicating the combustion of different carbon and sulphur species. At around 480°C, the combustion of polymeric carbon causes the evolution of CO_2. At 730°C, graphite is burned that is a constituent of the catalyst. Above 800°C, the weight curve and the SO_2 signal (brown curve) allow the exact quantification of the sulphur content. However, no further information on the nature of sulphur compounds can be obtained, because all sulphur species on the nickel catalyst are converted to sulphate under TPO conditions.

6.2 XANES

To obtain further insights, X-ray absorption spectroscopic studies have been carried out at the LUCIA beam-line of the Swiss Light Source (SLS) at PSI. The XANES part of the spectrum reveals element specific information on the oxidation state. XANES measurements focussing on the sulphur K-edge of active and deactivated catalyst sampled oxygen-free from the test reactor and subsequent comparison with XANES spectra for reference and model samples allowed identifying the nature of the sulphur species on the catalyst surface (see Figure 13). Whereas the active catalysts shows sulphur in form of sulphides (e.g. Ni_3S_2), the fully deactivated catalyst shows clear signs of organic sulphur.

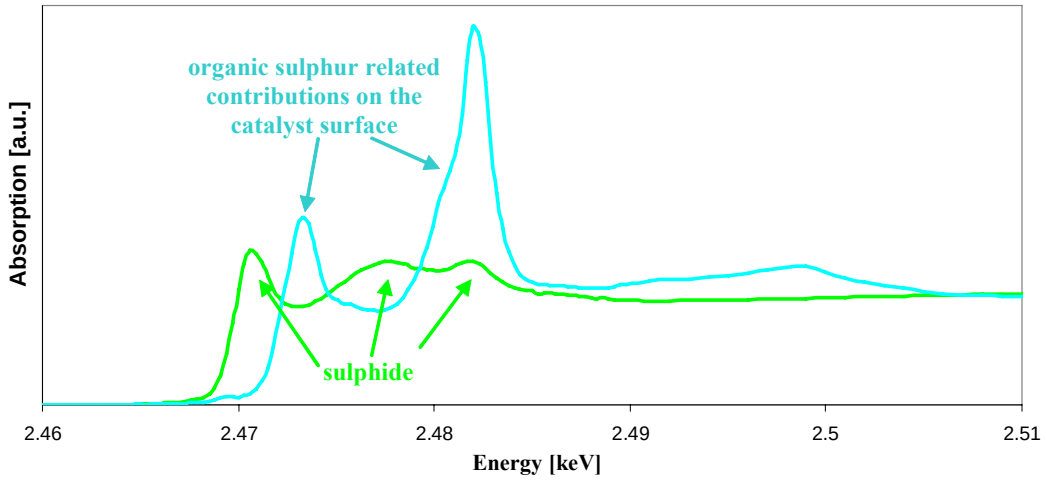

Figure 13 Sulphur K-edge XANES spectrum of active (green) and deactivated (blue) Ni/γ-Al_2O_3 catalyst from methanation experiments in Güssing/Austria the main focus of further

From the post-test analyses described above, different possible deactivation mechanisms can be derived:

- a sudden break-through of organic sulphur species,
- a sudden break-through of organic compounds (e.g. tars) which deactivate the catalyst by (polymeric) carbon deposition

If the amount of catalyst applied in the experiments is significantly higher than the amount needed to reach the thermodynamic equilibrium, also slow deactivation processes like poisoning by sulphur or hydrocarbon species can be thought of. The fifth possibility is a combination of the previous possibilities.

Therefore, a double strategy was applied. To check for slow deactivation processes, more catalyst samples were taken during the next experiments in Güssing.
Significant work was spent on the improvement of the desulphurization. Adequate tools for the identification and quantification of the sulphur species were needed. Furthermore, a catalyst for the hydrodesulphurization HDS of organic sulphur compounds was identified that could replace one of the ZnO-beds.
Even though there were strong indicators for sulphur poisoning, a contribution of carbon

deposition on the deactivation of the catalyst could not be excluded. The increase of C_2H_6 in the raw SNG points out the relevance of carbon deposition in this deactivation process. Therefore further investigations focused on understanding the role of carbon on the catalyst surface (see next section and chapter 7).

6.3 Catalyst characterisation by XPS analysis

The catalyst samples were crushed and pressed into pellets directly at the sample holder (without any glue or adhesive tape). XPS analysis of the industrially used catalyst samples was performed ex situ. Experiments with model reactions were carried out in-situ in the high pressure cell (HPC). The XPS measurements were done in an ESCALAB 220i XL electron spectrometer by using a non-monochromatic Mg Kα (1253.6eV) radiation twin source at a chamber pressure around $5x10^{-10}$ mbar. The electron energy analyzer was operated in the constant pass energy mode with pass energy 50 eV for survey scans and 20 eV for region scans. The quantification of the XPS spectra was carried out using the transmission function of the electron energy analyzer and the cross-sections calculated by Scofield. The binding energy (BE) was adjusted using the C1s transition placed at 284.5eV as well as Al2p transition placed at 119.0eV (characteristic BE of Al 2p in Al_2O_3). The conductivity of the samples was high enough to keep charging during the XPS measurement below a few eV (max. ~ 10eV).

Three sets of experiments were performed: a) analysis of samples (commercial catalyst) from the Güssing plant with differently operation modes ("Gasifier x"), b) HPC experiments using the commercial catalyst under "quasi in situ" conditions applying various gas compositions (including an artificial Güssing gas), and c) experiments using a home-made model catalyst. The experiments under b) and c) were made applying the following reaction conditions: 400°C, 1.5 bar abs., total flow: 8.0 ml_n/min.

The feed gas composition from the "artificial Güssing gas" as mimic of the real Güssing gas is presented in following table.

Component	%
H_2	13.0
CO	8.8
CO_2	6.2
H_2O	4.9
CH_4	3.3
C_2H_4	1.0
$C_2H_2/C_3H_6/C_2H_6$	0.5
Ar	62.3

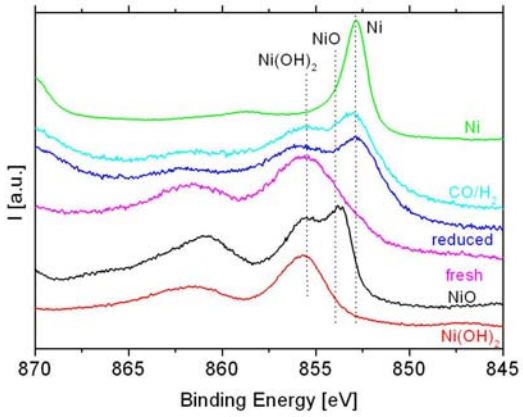

a)

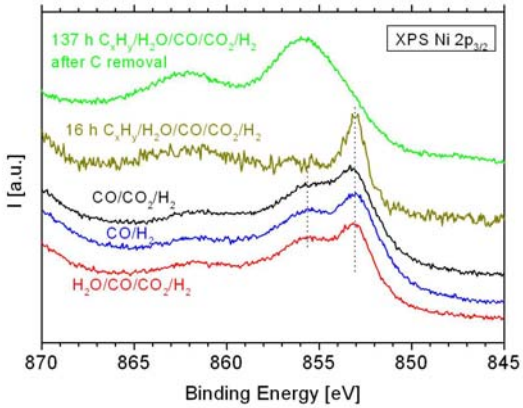

b)

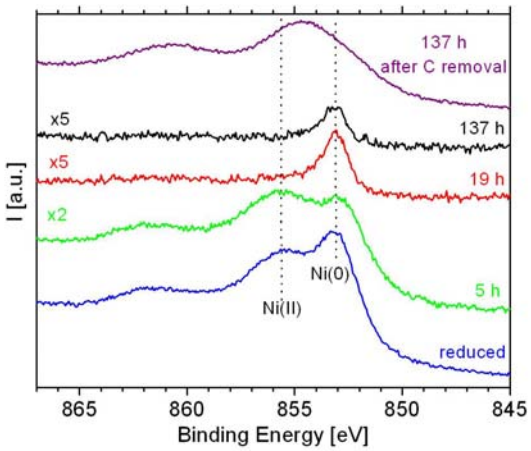

c)

Fig. 14 - Comparison of Ni reference spectra with spectra of surface species measured by XPS ($Ni2p_{3/2}$ region) during methanation runs over Ni/Al_2O_3 catalyst. a) Pure Ni, NiO and $Ni(OH)_2$ as well as fresh, reduced catalysts and after exposure to CO/H_2. – b) Comparison of Ni surface composition as function of the reactant concentration: $CO/CO_2/H_2$ - CO/H_2 -$H_2O/CO/CO_2/H_2$ - $C_xH_y/H_2O/CO/CO_2/H_2$ (16 h) and after mechanical removal of carbon (137h). – c) Surface changes during an extended run applying an artificial Güssing gas mixture.

The XP spectra of Figure 14 show that, after the initial applied reduction cycle, the surface Ni is not fully reduced. Various amounts of Ni^0 and Ni^{2+} are recorded. Exposure to various stoichiometric $CO/CO_2/H_2O/H_2$ gas mixtures (Fig 1b) reduces the catalyst only a bit more. Only in the presence of C_xH_y, the surface composition is altered.
In Fig. 1c) spectra from an extended reaction run are displayed. The first (bottom) spectrum shows the freshly reduced catalyst. During the run, the Ni signal is 1) decreasing in intensity, and 2) shifted only to Ni^0. After extended reaction times, an intense production of C was found on the catalyst. After the C removal, the topmost spectrum was recorded, showing that the catalyst surface (Ni/Al_2O_3) was basically not changed with respect to the reduced one, only Ni^0 signal is still present, but less intense.

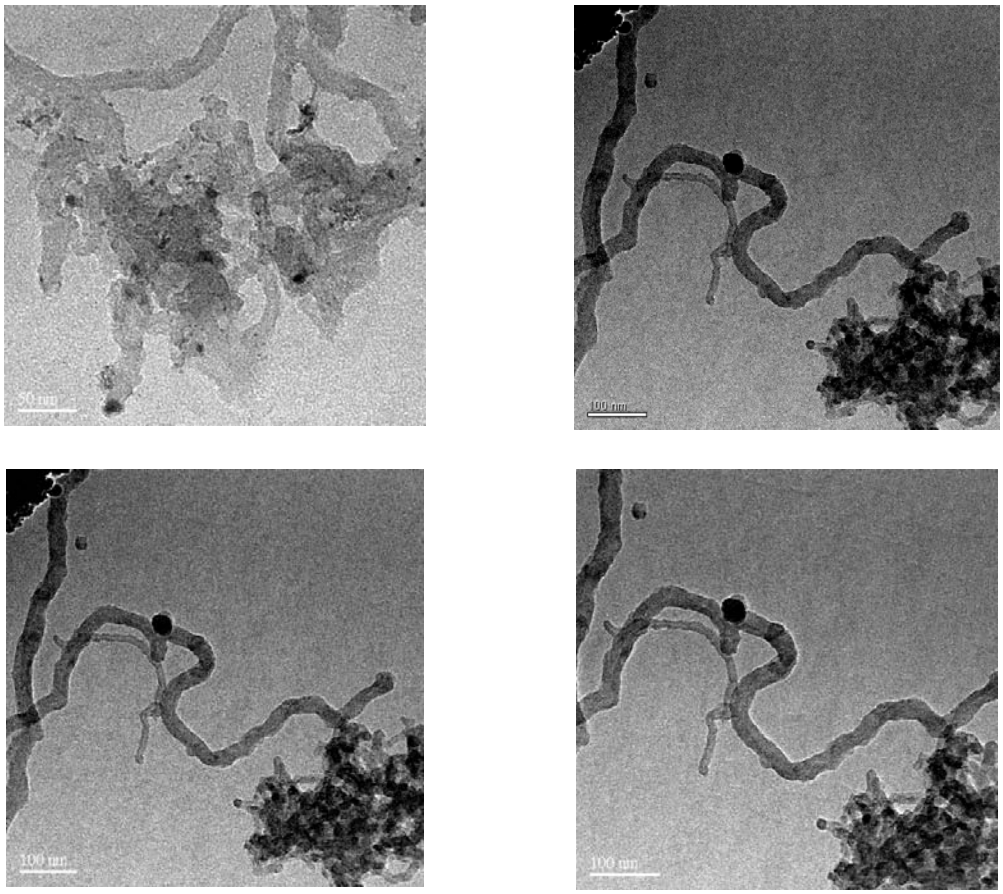

Fig. 15 HR-TEM of the commercial Ni/Al_2O_3 catalyst.

The removed carbon was analysed by HRTEM. The images are displayed in Figure 15. They clearly show the formation of pure carbon whiskers. Additional conglomerates (dark dots) were identified to be metallic Ni clusters, which is in accordance with the XPS findings. The connections between C-whiskers and Ni metal clusters indicate a Ni-detaching mechanism from the surface.

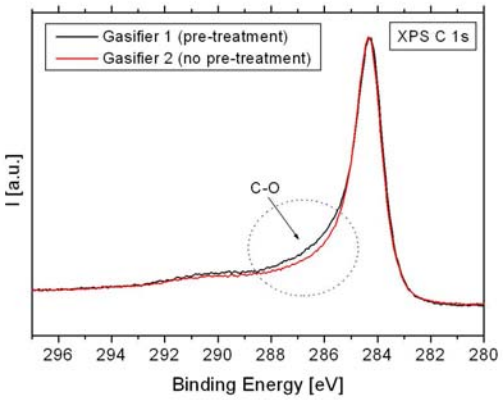

Fig. 16 Methanation over Ni/Al_2O_3 catalyst. – C 1s region from catalysts used in Güssing with two differently operation modes: 1) Gasifier 1 (catalyst pre-treated); 2) Gasifier 2 (catalyst no pre-treated).

Figure 16 shows the differences in the C1s region for two catalyst samples which were taken, when the set-up was operated with and without pre-treatment. Slight differences in region BE ~ 289-286eV are observed due to creation of C-O bonds after pre-treatment.

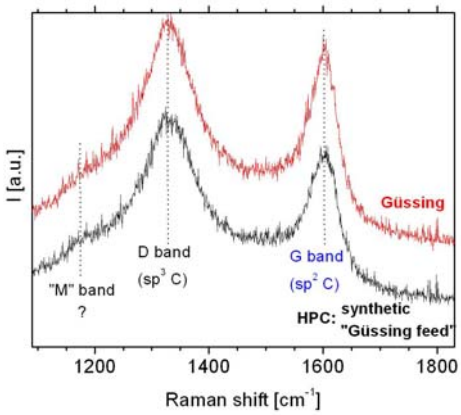

Fig. 17 Comparison of carbon Raman spectra from Ni/Al_2O_3 catalysts. Top: sample from the Güssing set-up. – b) sample from the HPC using the ”artificial Güssing feed”.

Figure 17 presents Raman results of the formed carbon on Ni/Al_2O_3 catalysts. The results show that in both cases (samples from the Güssing set-up and from the High Pressure Cell using an artificial “Güssing feed”) very similar type of C is formed. However, the C is disordered, with very small graphite-like domains (~2-3 nm). The “M” band, which is observed in both spectra, indicates the presence of C-C groups. It can be stated, that the presence of hydrocarbons in the feed enhances the formation of carbon at the surface. In case of a not-fluidised catalyst bed, carbon whiskers are formed. It is interesting to note that the carbon from the HPC and from the fluidised bed reactor in Güssing has the same composition. The carbon concentration has only a slight effect on the methanation activity due to the fact that nickel particles are detached from the surface and create cluster on the C-whiskers. The clusters can be quite thick and particularly consist of metallic Ni. With respect to the fluidised bed reactor used in Güssing, it would be interesting, how possible concentration gradients through the fluidised bed could prevent, stop, or even revert the Ni-detaching mechanism.

7. Axial gas phase concentration profiles in the methanation reactor

The aim of this investigation was to show the positive effect of fluidization on the methanation reaction by probing gas compositions inside the fluidized bed. Gas phase concentration profiles in the emulsion of the fluidized bed were taken by means of a moveable sampling probe. To assure stable methanation operation without deactivation, the fundamental phenomenon has been studied with a H_2/CO ratio of 3.

7.1 Experimental

The scheme of the setup (COALA) is shown in figure 18. This setup is designed for catalyst testing under realistic fluidized bed conditions. It consists of a 50 mm diameter fluidized bed reactor (1) with a diffuser at the upper end to control the discharge of fines. The gas is introduced via a non reactive porous metal plate. The temperature of the reactor is measured by a sidewise immersed fixed thermocouple about 5 mm above the porous metal plate (2) and controlled by cooling the outside reactor wall with air. Water produced by the methanation reaction is condensed and weighed (3).

The core of the setup is a moveable sampling probe (4) with a 2 mm Ø porous titanium plate at the tip. The probe is equipped with a thermocouple (5) at the tip to measure the ambient temperature. Driven by a linear motor, this probe is immersed axially from the top of the reactor into the catalyst bed. Spacers at two different heights assure the radial position of the probe. For the experiments where the probe is positioned outside the middle axis, different kinds of spacers are used. By means of a gas pump, a continuous flow of 10 ml/min is transported to the GC via an $MgSO_4$ adsorber for removal of the moisture (6). Gaseous products are analyzed online by a micro-gas chromatograph (μ GC) with two columns (Varian CP 4900; detector TCD, Columns MSA5, PPU) or mass spectrometer (MS) (VG ProLab Thermo ONIX).

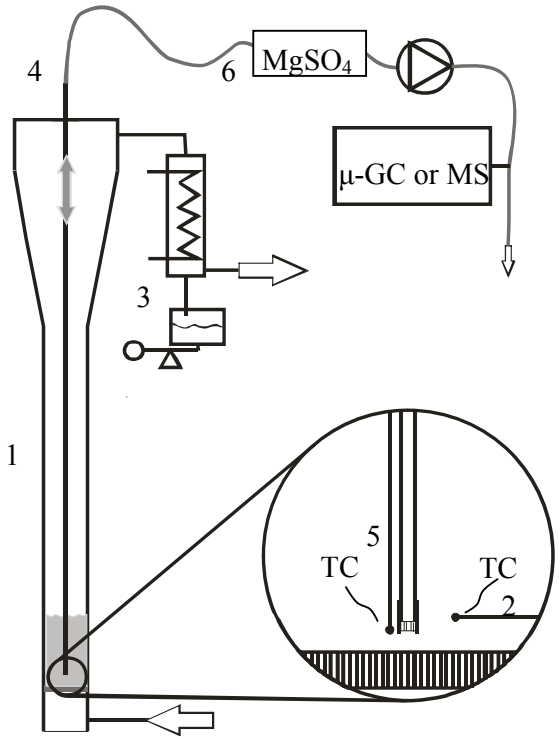

Fig. 18: Scheme of the Setup

For the experiments shown, 100 g of a commercial nickel on γ-Al_2O_3 catalyst were used. The reactor temperature was kept between 320-330°C and the pressure at 1.3 bars. The gas mixture consisted of 6 l/min H_2 and 2 l/min CO (H_2/CO = 3). As internal standard, additionally 2 l/min N_2 were added to the mixture to enable the calculation of molar flows from the μ GC results.
A typical experiment consisted of three similar runs where the sampling probe was moved with 20 steps up and 20 intermediate steps down. If the reaction conditions were stable and the three runs of one experiment were congruent, the data was considered as reliable. Before each set of experiments, the μ-GC was calibrated with calibration mixtures (±2 % relative error) at four concentration levels per gas species (H_2/CO/CO_2/CH_4/N_2). Only experiments on consecutive days were compared to minimize effects due to potential catalyst aging and changes of the GC performance. The experiments were repeated several times to assure the quality of the data.
At the start of the experiment the sampling probe was immersed with a back flush of helium to avoid clamping particles, and moved down to the porous plate (level zero). Then the helium back flush was stopped and the pump and the μ-GC were started. In the following, the sampling probe was moved up and down automatically by the linear motor (precision ± 0.125 mm).

7.2 Results and discussion

In figure 19, the measured concentration of a typical experiment with a H_2/CO ratio of 3 is plotted versus the reactor height. As the methanation reaction causes a contraction of the gas volume, the concentration profile is affected by changes of the total volume. The molar flows were derived the measured concentrations using N_2 as internal standard.

Bubbling fluidized beds are split into a dense phase (emulsion) and a phase of low solid density called bubbles (voids). The measurement in the bed represents mainly the gas concentration in the dense phase, as bubbles avoid the large hydrodynamic resistance from the immersed probe. In the freeboard, the gas passing the emulsion mixes with the gas from bubbles. Conversion in the bubbles is lower than in the emulsion. Mixing of the two gas streams (bubble, emulsion) at the outlet of the bed leads to a change in the concentrations (see figure 18 above 90 mm). Therefore, the standardization of the gas concentration differs between bed and freeboard, as not 100% of the N_2 passes the emulsion.

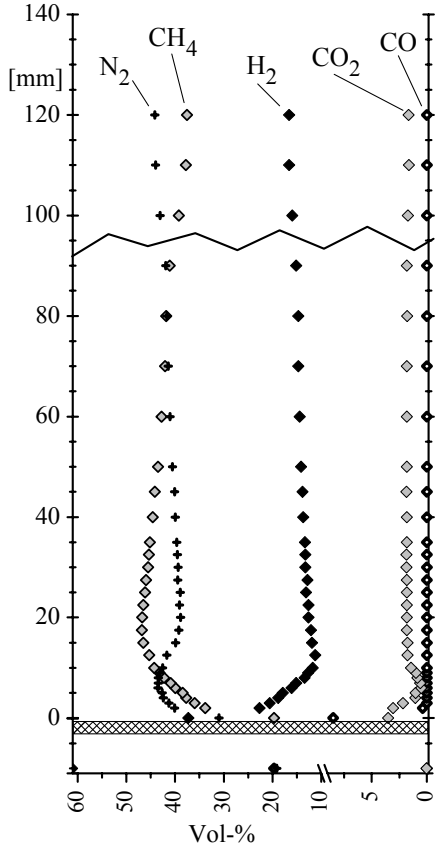

Fig. 19: Profile of the concentration in vol-% as measured by μ-GC at H_2/CO=3, 320°C and 1.3 bar; the gas composition of the inlet flow is H_2/CO/N_2: 6/2/2 l/min

The balances of the gas phase can be calculated for each axial position. As the amount of water is not measurable with the μ-GC, it is calculated from the missing O atoms. This assumption has been validated by MS measurements. Furthermore, the collected condensate was found to close the overall O-balance.

In Figure 20a, the four traces of the molar flows of the gases plus the calculated water flow are shown versus the height of the reactor. According to the temperature measurement, the end of the expanded bed is close to 100 mm. Next to the diagram is a list of the dominating reactions depending on the zone. Below the schematic representation of the porous plate below 0 mm, the molar flows of the educts are shown. The flows of CH_4 and CO_2 are zero the CO flow is 0.09 mol/min. The H_2 flow of 0.27 mol/min is not visible on this scale. The profile itself starts

at level zero, the lowest point the test probe can reach. Due to clamped particles under the test probe, the surface of the distributor plate is not reachable for the sampling probe.

In figure 20b, the carbon balance of the gas phase is shown. The values of the balance are the result of the comparison between the inlet composition and the gaseous C species measured with the sampling probe (eq. 4).

$$C_{balance}(x) = \Sigma_{\text{Call gaseous species reactor}} - C_{CO\ inlet} \qquad (4)$$

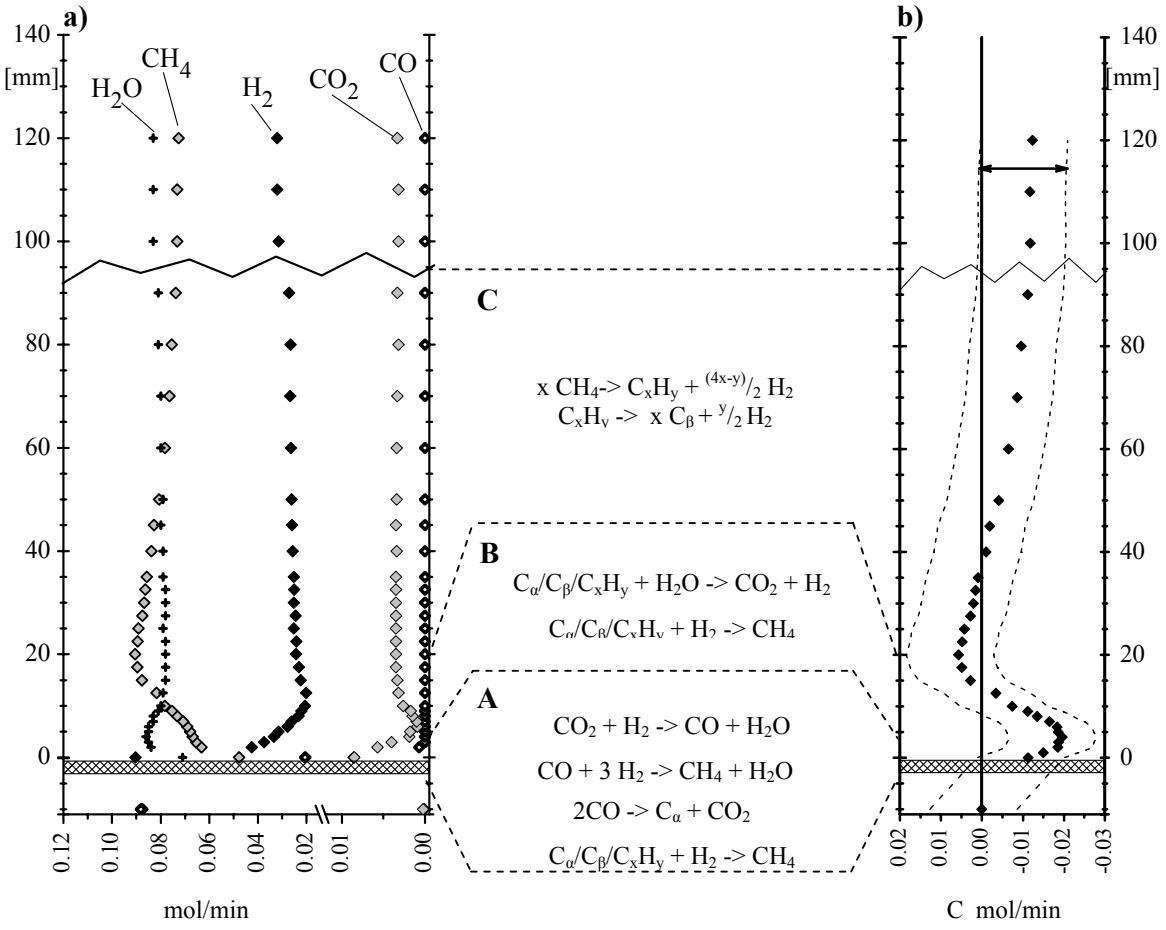

Fig. 20: Profile of molar flows (a) and the C-balance of the gas phase (b) in mol/min. The parallel traces in the C-balance represent the systematical measurement uncertainty due to relative errors of calibration gases. The dominating reactions in zones A, B and C are shown in between.

As the concentrations of the inlet mixture differ extremely from the concentrations in the emulsion, the relative errors of the four calibration gases have a strong impact on the C balance. Therefore, the exact Y position of the trace suffers from a significant systematically uncertainty, shown by the dotted lines parallel to the trace of the C balance. The relative differences within the carbon balance, i.e. the shape of the carbon profiles, however, are very reliable and were reproduced in all of totally 20 experiments.

The calculated carbon balance shows a carbon deficit above the bed of 0.01 mol/min which would result in a significant build up of solid carbon (1kg) over the running time of a series of 20 experiments. As the operation conditions were stable and no carbon was found in the filter, the real carbon balance must probably be around zero between 90 and 120 mm, i.e. the curve should be shifted up.

The gas phase profile and the C balance can be divided into three different zones; A, between level 0 and 5 mm including the range that is not reachable by the probe; B, between 5 and 20 mm and C, from 20 mm to the end of the bed at merely 100 mm.

Zone A

At the inlet of the bed, some reactions proceed so fast, that even at the deepest point the probe can reach, 75 % of the introduced carbon is converted into CH_4 and CO_2. Within the first five millimetres of the accessible bed, the methanation reaction and the Bouduoard reaction are dominating, causing an increase in temperature of about 40 °C. During this period, carbon deposition due to CO adsorption (most probably in form of adsorbed C_α) as visible in the carbon balance of the gas phase in figure 19b takes place. At about 5 mm, due to the high H_2 concentration and the decreasing amount of CO, the reverse WGSR starts to dominate, so that the CO_2 flow shows a minimum and the H_2O flow a maximum.

Zone B

Above the level of 5 mm, all carbon containing species in the gas phase increase. In addition to the hydrogenation of C_α, the gasification and subsequent methanation (eq. 5 and 6) and hydrogenolysis of less reactive carbon forms, C_β and coke (eq. 7), take place. The reactions are promoted by the high partial pressure of H_2 and water.

$$C_\beta\ ,\ C_xH_y + H_2O \rightarrow CO_2 + H_2 \qquad (5)$$

$$CO_2 + 4\ H_2 \rightarrow CH_4 + 2\ H_2O \qquad (6)$$

$$C_\beta\ ,\ C_xH_y\ +\ H_2 \rightarrow CH_4 \qquad (7)$$

As a result, the CO_2 and CH_4 flows increase whereas water and hydrogen are consumed. At a height of 20 mm, the molar flow of CH_4 has its maximum which is clearly above the chemical equilibrium of the gas mixture fed to the reactor.

The characteristic of the carbon balance in the gas phase reflects this situation; the amount of gaseous carbon exceeds by 20 % the initial amount introduced as CO. To enable this strong increase of gaseous carbon species, the catalyst passing through this zone must be covered with a pool of excess carbon species. This pool of solid carbon species (C_α, C_β and coke) on the catalyst particles evokes a change of the gas composition and consequently the chemical equilibrium.

Zone C

The high amount of carbon species in the gas originates from out of the solid carbon pool by reactions 2 and 4, driven by the high partial pressures of H_2O and H_2. Above 20 mm, a low H_2 concentration leads to slow methane decomposition. As the H_2 flow does not increase stoichiometrically, the formation of coke is likely.

Freeboard

When the gas from the emulsion leaves the bed mixing with the gas out of bubbles occurs. The bubbles pass the bed with less contact to the catalyst; therefore, the concentrations at the end differ from the gas concentrations in the emulsion phase (see figure 20). Subsequently, a change in the gas concentration profile takes place. CH_4 and CO_2 concentrations decrease and the concentration of H_2 increases. The present setup does not allow determining the gas phase concentration in the bubbles or the mass transfer rates between bubbles and emulsion phase. Therefore, quantifying the influence of the gas from bubbles on the final gas concentration is not possible, as not only the amount of gas in the bubbles matters but also reactions in the wake of the bubbles and the mass transfer between emulsion and bubbles.

In the freeboard, differences between the measured flow and the flow expected from the chemical equilibrium composition of the initially fed gas mixture can be observed mainly for H_2 and for CH_4 and CO_2.

Carbon exchange processes

The rates of the all reactions depend strongly on the reactivity of the individual C species. Whereas reactions via C_α are very fast and close to the equilibrium, reactions via the less reactive C_β and coke are most likely kinetically limited. Thus, the gas concentration profile is close to the chemical equilibrium of the actual gas mixture at almost any level. Parallel, the overall amount of C in the gas is changed. Additionally, the amount of hydrogen can change via the shift between coke and C_β.

To visualize the exchange processes between the gas phase of the emulsion and the catalyst, three zones of the gas phase A, B and C are shown in figure 21. The gas within the defined zones is exchanging carbon with the solid phase. The amount of carbon on the catalyst is considered to be high compared to the exchanged amount of carbon. In each of the zones, a net C flow exist (indicated by the stronger arrows), superimposing the effect of processes in the opposite direction.

Zone A: Between 0 and 5 mm, C_α is formed due to CO dissociation. Even though hydrogenation and gasification of coke and C_β takes place as well, the net flow is directed to the solid phase.

Zone B: Between 5 and 20 mm, the hydrogenolysis and gasification by H_2O of all forms of C-deposits (C_α, C_β and coke C_xH_y) dominates, leading to a net C flow to the gas phase.

Zone C: From 20 mm until the end of the bed, the dissociation of excess methane dominates, coke is formed and the C pool is refilled.

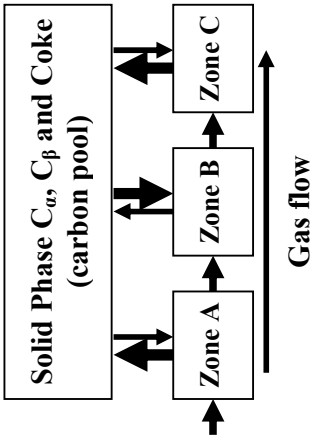

Fig. 21: Scheme of the carbon exchange processes between the gas phase of the emulsion and the carbon pool (solid carbon immobilized on the catalyst particles)

Conclusions

Reason for the internal regeneration during the methanation reaction is the permanent carbon exchange between a solid carbon pool on the catalyst surface and the gas phase. As in bubbling fluidized bed reactors the zones of deposition and removal of solid carbon are locally separated, the moving catalyst can act like a "buffer". This ability to compensate high carbon loads locally is one reason for the reduced tendency of fluidized bed methanation reactors towards excess carbon deposition and subsequent deactivation. When equilibrium between the permanent loading and unloading of the catalyst with carbon is assured, the activity of the catalyst is stable.

The methanation reactor is structured into three different zones.

- Predominantly carbon deposition by CO adsorption at the inlet zone;
- Predominant gasification and hydrogenation of carbon deposits in the following zone;
- Predominant coke formation by methane decomposition in the upper part of the bed.

These processes lead to a permanent C pool on the catalyst that is several times larger than the amount of gas phase carbon present in the reactor. The existence of such a C pool influences the reactions and the chemical equilibrium by changing the local atomic composition.

In combination with the particle movement the exchange between gas phase and catalyst results in net carbon fluxes in three principal directions; from centre of the bed to the rim of the bed, from the inlet zone A to the middle zone B and from the final zone C to the middle zone B.

Even though the characteristic of the profiles will change with different reactor geometry, the principal effects will remain. To sustain the promoting effect during the scale up of the reactor, attention towards proper fluidization must be paid. In this context, the prevention of a build-up of unreactive C_β is crucial. Otherwise, a slow decay of the activity will take place.

8. Experiments including the HDS unit in 2005

The experimental work in Güssing in 2005 focused the introduction of a HDS (hydro-desulphurization) step into the set-up. The first of the two ZnO absorber beds was replaced by a HDS catalyst bed. More Ni-catalyst samples were taken during the experiments and analysed by TPO which allowed quantifying both, carbon and sulphur, deposition. Additionally, an analytical tool for measuring the total sulphur content in the gas was set-up, i.e. a Sulphur Chemoluminiscence Detector (SCD) system.

8.1 Overview over the experiments

Cosyma_5

The first experiment including the HDS followed the conditions of Cosyma_3 and Cosyma_4 and was dominated by cautious steps to explore the performance and the limitations of the HDS. Whereas stable running of the HDS was achieved, the experiment did reproduce the previous catalyst lifetime of about 200 h.

Cosyma_6

The next experiment including the HDS was carried out with a doubled space velocity to investigate the effect of higher space velocity on the carbon deposition. However, this experiment was facing several technical problems, especially trouble with the gas/water separation unit after the fluid bed methanation reactor leading to partial flooding of the set-up. In total, 67 hours of stable run were achieved before the catalyst deactivated.

Cosyma_7

The next experiment was started after solving the technical problems with the gas/water separation unit. In order to ensure that the technical problems during Cosyma_6 were not the reason for the short catalyst live time, test conditions in Cosyma_7 were identical to Cosyma_6. Without major technical issues, the catalyst was stable for 72 hours.

Cosyma_8

No data are available as the test rig was flooded with water and test has to be stopped.

Cosyma_9

In parallel to the campaigns performed in Güssing, an analytical tool for on-line measurement of the total sulphur content in the gas was set-up, i.e. a Sulphur Chemoluminiscence Detector (SCD) system was developed at PSI. With this new tool, it should be possible to understand why previous experiments including the HDS did not show significant progress. The SCD tool for measuring the total sulphur content in the gas was installed in Güssing in the COSYMA installation. The developed SCD system allows to measure the performance of the HDS and the subsequent ZnO bed and therefore to optimize their working conditions of the gas cleaning during the experiment. Thanks to the on-line measurement of the total sulphur content, it could be easily shown, that, without the optimization of the HDS step, the sulphur flux to the methanation was more or less unchanged and therefore the HDS was not active. By improving the operation conditions of the HDS and halving the sulphur flux to the methanation, the time of stable catalyst run could be increased by more than 60% to 112 hours.

8.2 Results of TPO analyses and discussion

During all four experiments, catalyst samples were taken and subsequently analysed by TPO. As shown in Figure 22, especially the results of the sulphur quantification were very interesting.

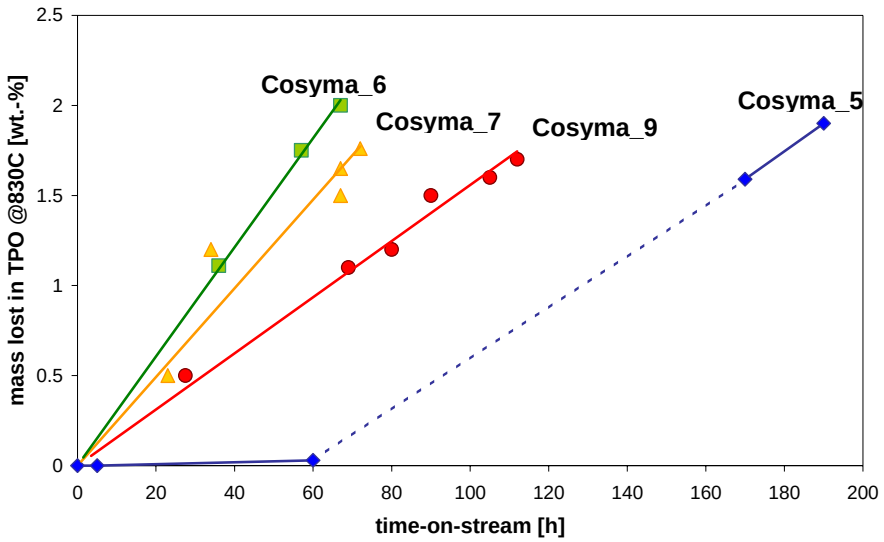

Figure 22 Mass lost in TPO analysis at 800ºC for catalyst samples from different Cosyma runs

During, the first 60 hours of Cosyma_5, only small amounts of sulphur were deposited on the catalyst, while the deactivated catalyst shows a significant sulphur loading. It can be speculated, that the sulphur content of the HDS catalysts was increasing during this period, leading to lower sulphur breakthrough onto the methanation catalyst.

Such a transitorily behaviour was not observed again. For the experiments 6 and 7, the space velocity was doubled. In these two experiments, it is clearly visible that the sulphur content of the samples increases linearly with time. The slope of the increase is about double of that found for Cosyma_5, but the sulphur content of the deactivated catalyst is about the same. This clearly hints on a poisoning of the catalyst with always the same, low concentration of sulphur species that was not removed by the HDS/ZnO combination.

The final prove for sulphur poisoning is the fact that in the experiment Cosyma_9, the space velocity was the same as in Cosyma _6 and _7, but the slope of the sulphur content in the catalyst samples was decreased significantly, and the duration of the experiment was increased consequently.

Therefore, it can be said that minimizing the remaining sulphur concentration in the gas is the key for longer catalyst lifetime.

III. Conclusions

The thermodynamic analysis and modelling of the process chain from biomass such as wood and straw to SNG results in the following conclusions:

- Based on the available data for raw gas composition (producer gases as well as syngases) a chemical efficiency for the whole process from biomass to SNG of 65% seems realistic.
- The requirements of H-gas quality according to the rules of the DVGW 260 can be fulfilled.
- The calculations identify a suitable temperature of up to 400 °C for high pressure applications and around 300 °C for atmospheric pressure methanation.
- To maximise the efficiency for the SNG production the heat management of gasification, gas processing and methanation process unit is a prerequisite.

The evaluation of raw gases for their suitability for SNG synthesis is a difficult task without experimental prove. Nevertheless, the thermodynamic considerations can give some criteria for the compatibility of different gasification systems with the methanation unit. The following conclusions can be drawn from the systems analysis so far:

- At equal chemical efficiency of the gasification systems, producer gases with a high content of methane are preferable for the production of SNG for several reasons. The overall chemical efficiency is increased and the challenge of cooling the methanation reactor is lowered as the heat loss in the synthesis unit decreases.
- The content of Nitrogen in the raw gas should be below 0.5%
- Concerning the carbon deposition on the methanation catalyst raw gases from entrained flow gasifiers have an advantage as the level of tars and higher hydrocarbons are low and consequently the carbon deposition risk is low. Otherwise, the tars must be removed from the raw gas in an additional operation unit to protect the catalyst.

The analysis showed that optimization of the gasification has the highest potential to improve the overall process. The goal of an ideal gasification system for SNG is low temperature gasification with high chemical efficiency, producing a methane-rich and nitrogen-free gas with low tar content. The optimization potential in the synthesis section is rather small as the thermal losses are depending greatly on the raw gas composition.
However, as a SNG production plant does feature more than these three operation units discussed above, technical concerns might dominate thermodynamic arguments. For a final accounting all energy flows must be considered.

For proving the concept of SNG production from FICFB gasifier producer gas under real conditions, the mobile container-based system for methanation (COSYMA) was set up.
In the first experiments, the set-up proved its robustness. The control unit met the demands for operator convenience and safety. The monitoring and control of the setup during the periods of

unmanned operation via internet proved to be a valuable tool. Compared to the campaign in 2003, the quality of the analytics was improved, so that the atomic balances are closed to 98%.
However, even though the results from 2003 were reproduced in the experiments Cosyma_3 and Cosyma_4, the goal of 1000 hours of operation was not reached so far. Subsequent post-test analysis of the deactivated catalyst by X-ray Photoelectron Spectroscopy (XPS) showed deposition of carbon and sulphur on the surface. As an important step towards understanding the mechanism of the deactivation, XANES-measurements (X-ray Absorption Near Edge Structure) at the Swiss Light Source (SLS) and analysis of catalyst samples by XPS and Temperature Programmed Oxidation (TPO) allowed determining the type of both carbon and sulphur species on the catalyst.
In-situ measurements of the axial gas phase concentration profiles showing strong carbon exchange processes between the catalyst and the gas phase proved the regenerative effect of fluidization on catalysts in methanation reactors.
In further experiments in Güssing, a HDS-catalyst was introduced in order to improve the gas cleaning. TPO analyses from Ni-catalyst samples of these experiments showed a poisoning of the catalyst with always the same, low concentration of sulphur species that was not removed by the HDS/ZnO combination. Optimizing the HDS performance and therefore minimizing the remaining sulphur concentration in the gas turned out to be the key for longer catalyst lifetime.
Future work will evaluate the possibility of further optimization of the HDS step and of alternatively introducing a suited scrubber process for the elimination of organic sulphur compounds.

Generally, it can be stated, that the Container based System for Methanation (COSYMA) is a valuable tool for field experiments with producer gas derived from an industrial biomass gasifier. Due to the flexibility of the setup design specifications for the scale up can be generated. Furthermore, the expected chemical efficiency of an industrial size link-up of a gasifier with the methanation can already be predicted.
For the tests at the FICFB gasifier, a CO conversion of > 98% and a conversion of aromatic hydrocarbons of 99% were calculated from the measured data. Assuming a cold gas efficiency of 70% for the gasifier, the chemical efficiency for the overall process “wood to SNG” is expected to be around 60 %. Although there is further potential in the optimization of the interaction of gasifier and methanation, the feasibility of SNG production from wood derived producer gas can be considered as successfully demonstrated under real conditions with the long duration test over 1000 h catalyst on stream (proof of concept).

IV. References

DVGW, *G 260 Gasbeschaffenheit -Arbeitsblatt-*. 2000.

DVGW, *Nutzung von Gasen aus regenerativen Quellen in der öffentlichen Gasversorgung -Arbeitsblatt-* -.

K. Hedden, Anderlohr, A., Becker, J., Zeeb, H.-P., and Cheng, Y.-H., *Gleichzeitige Konvertierung und Methanierung CO-reicher Gase*. Forschungsbericht Uni Karlsruhe T 86-044. 1986.

L. Devi, Ptasinski, K.J., Janssen, F.J.J.G., van Paasen, S.V.B., Bergman, P.C.A., and Kiel, J.H.A., *Catalytic decomposition of biomass tars: use of dolomite and untreated olivine.* Renewable Energy, 2005. **30**(4): p. 565-587.

S. Ramesohl, Arnold, K., Kaltschmitt, M., Hofmann, F., Plättner, A., Kalies, M., Lulies, S., Schröder, G., Althaus, W., Urban, W., and Burmeister, F., *Analyse und Bewertung der Nutzungsmöglichkeiten von Biomasse*. 2005, Wuppertal Institut für Klima Umwelt Energie, Institut für Energetik und Umwelt gGmbH, Fraunhofer Institut Umwelt-, Sicherheits-, Energietechnik (UMSICHT), Gaswärme-Institut e.V. Essen.

M. Seemann, Biollaz, S., Schaub, M., Aichernig, C., Rauch, R., Hofbauer, H., and Koch, R. *Methanation of biosyngas and simultaneous low-temperature reforming: First results of long duration tests at the FICFB gasifier in Guessing* in *14th European Biomass Conference & Exhibition. Biomass for Energy, Industry and Climate Protection* 2005 Paris, France.

C.A. T.Proell, H.Hofbauer, R.Rauch. *Coupling of Biomass Steam Gasification and an SOFC - Gas Turbine Hybrid System for Highly Efficient Electricity Generation* in *ASME Turbo Expo 2004: Power for Land, Sea, and Air*. 2004. Vienna, Austria.

Generator Gas. 3rd ed, ed. S.A.o. Engeneering. 1950, Golden, CO: Biomass Energy Foundation Press.

A. Kaup, *Small Scale Gas Producer-Engine Systems*, Golden, CO: Biomass Energy Foundation Press.

N.A. Skov and Papworth, M.L., *The Pegasus unit*. 3rd ed. 1974, Golden, CO: Biomass Energy Foundation Press.

D. Kirmse, Lysk, S., Kather, A., and Scheffknecht, G., *Operating experience with the two 800 MW steam generators in power plant Schwarze Pumpe.* VGB Kraftwerkstechnik (German Edition), 2000. **80**(6): p. 29-38.

W. Eckert and Weinstock, M., *The power plant Schwarze Pumpe.* Elektrizitaetswirtschaft, 1998. **97**(13): p. 61-2, 64, 66, 68.

H. Rehwinkel, Kmoch, G., and Schingnitz, M., *GSP entrained gasifier converts salty lignite.* Modern Power Systems, 1990. **10**(5): p. 39-42.

B.M. Wolf, *BIO-METHANOL AS A FUEL AVAILABLE FROM REGIONAL SOURCES*, C.I. GmbH, Editor. 2001: Freiberg. http://www.choren.com.

K. Stahl, Waldheim, L., Morris, M., and Bengtsson, S. *CHRISGAS PROJECT – CLEAN HYDROGEN-RICH GAS THROUGH BIOMASS GASIFICATION AND HOT GAS UPGRADING*. in *14th European Biomass Conference & Exhibition. Biomass for Energy, Industry and Climate Protection* 2005. Paris, France.

S. Albertazzi, Basile, F., Brandin, J., Einvall, J., Hulteberg, C., Fornasari, G., Rosetti, V., Sanati, M., Trifiro, F., and Vaccari, A., *The technical feasibility of biomass gasification for hydrogen production.* Catalysis Today, 2005. **106**(1-4): p. 297-300.

C. Pfeifer, Rauch, R., and Hofbauer, H., *In-bed catalytic tar reduction in a dual fluidized bed biomass steam gasifier.* Industrial & Engineering Chemistry Research, 2004. **43**(7): p. 1634-1640.

H.R. Hofbauer, R.; Loeffler,G.; Kaiser,S.; Fercher,E.; Tremmel,H.;. *Six Years Experience with the FICFB-Gasification Process* in *12th European Conference and Technology Exhibition on Biomass for Energy, Industry and Climate Protection*. 2002. Amsterdam.

R. Rauch. *Steam Gasification of Biomass at CHP Plant in Guessing - Status of the Demonstration Plant* in *2nd World Conference and Technology Exhibition on Biomass for Energy, Idustry and Climate Protection*. 2004. Rome, Italy.

L.C.R.d. Sousa, *Gasification of wood, urban wastewood (Altholz) and other wastes in a fluidised bed reactor*. 2001: Zürich.

V. Publications

T.J. Schildhauer, R.P.W.J. Struis, S.M.A. Biollaz, Post-test analysis of deactivated methanation catalyst by XANES and TPO, Scientific Report Volume 3, Paul Scherrer Institut Villigen, Switzerland (2006)

M.C. Seemann, T.J. Schildhauer, S.M.A. Biollaz, S. Stucki and A. Wokaun, The regenerative effect of catalyst fluidization under methanation conditions, Applied Catalysis A: General, Volume 313, Issue 1, 25 September 2006, Pages 14-21

I. Czekaj, F. Raimondi, J. Wambach, S. Biollaz, A. Wokaun. Characterization of surface processes at Ni-based catalyst during the methanation of synthesis gas: X-ray photoelectron spectroscopy (XPS), Applied Catalysis A: General, Volume 329, 2007, Pages 68-78.